Frontal cortex lipid alterations during the onset of Alzheimer's disease

Marta **Moreno-Rodriguez**[a], Sylvia E. **Perez**[a], Jonatan **Martinez-Gardeazabal**[b], Ivan **Manuel**[b], Michael **Malek-Ahmadi**[c], Rafael **Rodriguez-Puertas**[b]*, Elliott J. **Mufson**[a,d]*

a. Department of Translational Neuroscience, Barrow Neurological Institute, Phoenix 85013, AZ, USA.
b. Department of Pharmacology, Fac. of Medicine and Nursing, University of the Basque Country. 48949 Leioa, Spain.
c. Banner Alzheimer's Institute, Phoenix, 85006, AZ, USA
d. Departments of Translational Neuroscience and Neurology, Barrow Neurological Institute, Phoenix 85013, AZ, USA.

*****Both authors contributed equally to the overall direction and planning of the research

Running Title: Frontal cortex lipid activity in Alzheimer's disease

Corresponding author:

Elliott J. Mufson, Ph.D.
Director, Alzheimer's Disease Research Laboratory
Greening Chair in Neuroscience
Professor, Department of Neurobiology
Barrow Neurological Institute
350 W. Thomas Rd.
Phoenix, AZ 85013
Phone: 602-406-8525
Fax: 602-406-8520
email: elliott.mufson@barrowneuro.org

Abstract

Background: Although sporadic Alzheimer's disease (AD) is a neurodegenerative disorder of unknown etiology, familial AD (FAD) is associated with specific gene mutations. A commonality between these forms of AD is that both display multiple pathogenic events including cholinergic and lipid dysregulation.

Objective: We aimed to identify the relevant lipids and the activity of their related receptors in the frontal cortex, correlating them with cognitive function throughout the progression of AD.

Methods: MALDI-Mass Spectrometry Imaging (MSI) and functional autoradiography was used to evaluate the distribution of phospholipids/sphingolipids and the activity of cannabinoid 1 (CB_1), sphingosine 1-phosphate 1 ($S1P_1$) and muscarinic M_2/M_4 receptors in the frontal cortex (FC) of people that come to autopsy with premortem clinical diagnosis of AD, mild cognitive impairment (MCI) and no cognitive impairment (NCI).

Results: MALDI-MSI revealed an increase in myelin-related lipids, such as diacylglycerol (DG) 36:1, DG 38:5 and phosphatidic acid (PA) 40:6 in the white matter (WM) in MCI compared to NCI, and a downregulation of WM phosphatidylinositol (PI) 38:4 and PI 38:5 levels in AD compared to NCI. Interestingly, elevated levels of phosphatidylcholine (PC) 32:1, PC 34:0, and sphingomyelin (SM) 38:1 were observed in discrete lipid accumulations in the FC supragranular layers during disease progression. Muscarinic M_2/M_4 receptor activation in layers V-VI decreased in AD compared to MCI. CB_1 receptor activity was upregulated in layers V-VI, while $S1P_1$ was downregulated within WM in AD relative to NCI.

Conclusions: FC WM lipidomic alterations are associated with myelin dyshomeostasis in prodromal AD, suggesting WM lipid maintenance as a potential therapeutic target for dementia.

Keywords: Alzheimer's disease, MALDI-MSI, lipidomic, cholinergic, mild cognitive impairment, muscarinic receptor, autoradiography

INTRODUCTION

Alzheimer's disease (AD) is the most common type of dementia, characterized by a progressive deterioration of cognitive function. In addition to the beta-amyloid (Aβ) plaques, neurofibrillary tangles and central cholinergic deficits, clinical and epidemiological investigations have linked disrupted lipid metabolism with the pathogenesis and progression of AD [1]. Previous studies using lipid extractions have shown decreases in cortical polyunsaturated fatty acids (PUFA) and monounsaturated fatty acids (MUFA) in AD [2]. Docosahexaenoic acid (DHA) and arachidonic acid (AA), which are the most abundant brain PUFAs are downregulated in hippocampus [3], cortical levels of phosphatidylcholine (PC), phosphatidylinositol (PI) and phosphatidylethanolamine (PE) are reduced, while diacylglycerols (DG) increase [4, 5] in AD. Sphingomyelin (SM), galactosylceramides, and sulfatides, important components of myelination, are lower in cortical areas in AD and subjects with very mild dementia [6-9]. In addition, a loss of ceramide synthase 2, that produces very long acyl chain lipids of myelin, precedes neurofibrillary tangle pathology in temporal and frontal cortical grey matter (GM) in AD [10]. Despite evidence of lipidomic dysregulation, its role in the pathogenesis of AD remains unexplored. During the past several years the development of matrix-assisted laser desorption/ionization mass spectrometry imaging (MALDI-MSI), which is capable of the simultaneous visualization of the spatial distribution of hundreds of thousands of lipids in a label-free manner [11-13] provided a new tool for the investigation of lipids in AD. For example, MALDI-MSI was employed to investigate the spatial correlation of lipids within Aβ plaques [14, 15] and to discover novel therapeutic approaches centered around the modulation of lipid signaling in AD animal models [16-18]. The application of MALDI-MSI based lipidomic research

reported a reduction of sulfatides, myelin specific lipids in the FC [19] and a decrease of DHA-containing PC in temporal gray matter of late-stage AD patients [20, 21].

The FC, a component of the default mode network (DMN) [22], which plays a key role in the modulation of episodic memory, displays cholinergic deficits and alterations in choline-containing lipids (e.g., PC and SM) in AD [23, 24]. However, the relationship between lipid and cholinergic dysregulation during the onset of AD remains unknown. Disruption in lipid homeostasis may lead to cholinergic dysfunction, due changes in phospholipid and sphingolipid pathways that are critical for cell membrane repair and production of the neurotransmitter acetylcholine (ACh), which are affected in AD [25, 26]. Since cannabinoid 1 (CB_1) and sphingosine 1-phosphate 1 ($S1P_1$) receptors are the most widespread lipidic neuromodulators within the central nervous system and their endogenous ligands are derived from membrane lipid precursors, changes in the activity of these receptors likely play a key role in the modification of lipid homeostasis [27-29], which may be altered in AD. In this regard, CB_1 activity is increased following basal forebrain cholinergic denervation [30] and the modulation of the release of ACh in rat cortex [31], suggesting an interaction between cannabinoid and cholinergic systems resulting from cannabinoid activation via muscarinic receptors [32, 33]. Although FC CB_1 receptor activity is alter in AD [34] and even upregulated in the early stages of the disease [35, 36], others report no change or a decrease in sporadic AD [37, 38]. However, lysophospholipid $S1P_1$, which is also activated after cholinergic muscarinic signaling [33] is decreased in the superficial layers of the FC in severe AD [39]. Therefore, the aim of the present study was to identify early lipid dysregulation within grey and white matter (WM) and their relationship with CB_1, $S1P_1$ and muscarinic receptor activity in the FC during the onset of AD, using MALDI-MSI and functional autoradiography.

MATERIALS AND METHODS

Subjects

The study included 15 cases with a *premortem* clinical diagnosis of no cognitive impairment (NCI, n = 5; 86.27 ± 4.8 years), mild cognitive impairment (MCI, n = 5; 83.32 ± 7.4 years) and mild to moderate AD (AD, n = 5; 92.04 ± 5.4 years) from the Rush Religious Orders Study (RROS) and 6 younger-aged controls (YAC, 68.83 ± 7.9 years) non cognitively impaired Braak stage 0 cases from the Biobank of the Basque Country and Asturias Central University Hospital (see Table 1).

The Human Research Committees of Rush University Medical Center and Dignity Health approved this study and written informed consent for research and brain autopsy was obtained from the participants or their family/guardians. The YAC samples were obtained at autopsy following informed consent in accordance with the ethics committees of the University of the Basque Country (UPV/EHU) (CEISH/244MR/2015/RODRIGUEZ PUERTAS), following the Code of Ethics of the World Medical Association (Declaration of Helsinki) and warranting the privacy rights of the human subjects.

Clinical and Neuropathological Evaluation

The demographic, clinical and neuropathological characteristics of the cases provided by the RROS and the Biobank of the Basque Country and Asturias Central University Hospital are presented in Table 1. Although a similar detailed clinical evaluation was not available for the YAC cases, there was no evidence of cognitive difficulties or neurological disease in their medical records. Clinical criteria for NCI, MCI, and AD RROS cases have been reported in numerous previous publications [40, 41]. Here we provide an overview of the RROS clinical evaluation process. The RROS clinical evaluation was designed to determine the presence of dementia and its etiology, with particular attention paid to Alzheimer's disease (AD). Examination of medical history included uniform, structured questions about cognitive decline, stroke, Parkinson's disease, head injury, tumor, depression, and other medical problems. Medications used

within the previous 14 days of examination were reviewed. A uniform structured neurologic examination was carried out by trained nurse clinicians and neuropsychology technicians administered a battery of cognitive tests. Tests were chosen to assess a range of cognitive tasks with an emphasis on those affected by aging and AD (e.g., Mini-Mental State Examination (MMSE) [42], the CERAD neuropsychological measures: Verbal Fluency, Boston Naming, Word List Memory, Word List Recall and Word List Recognition [43], oral version of Symbol Digit Modalities Test [44], Logical Memory (Story A) and Digit Span subtests of the Wechsler Memory Scale-Revised [45], Complex Ideational Material [46], Judgment of Line Orientation [47], and subsets of items from the Standard Progressive Matrices [48]. A caveat of neuropsychological tests is that they do not measure cognition uniformly across different levels of education, educationally adjusted cut points were used for rating impairment on each test based on prior test use and existing reports in the literature. A computer algorithm applies these cut points uniformly and converted each participant's score into deficit ratings in five cognitive domains (orientation, attention, memory, language and perception) [49, 50]. An impaired score was developed for each domain that entailed dysfunction on several tests within that domain. A board-certified neuropsychologist, blinded to a participant's demographics, clinical data except education, occupation, and information about sensory or motor deficits used these findings to summarize deficits in each of the five cognitive domains as probable, possible or not present. For those cases with borderline dementia an opinion regarding the probability of dementia and AD is made by the neuropsychologist. A clinical diagnosis was then made by a board-certified neurologist with expertise in the evaluation of older people in combination with a neuropsychologist's opinion of cognitive impairment and the presence of dementia. The diagnosis of dementia and AD was made based upon the recommendations of the joint working group of the National Institute of Neurological and Communicative Disorders and the Stroke and the Alzheimer's Disease and Related Disorders Association (NINCDS/ADRDA) [51]. MCI criteria are compatible with those used by

many others to describe persons who are not cognitively normal but fail to meet accepted criteria for dementia [52-54]. Here, MCI was defined as those persons rated as impaired on neuropsychological testing by the neuropsychologist but were not determined to be demented by the examining neurologist. Average time from the last clinical evaluation to death was ~ 8 months.

Postmortem neuropathology for the RROS cases was performed as reported previously [41, 55], which included Braak staging [56], NIA-Reagan criteria [57], and the Consortium to Establish a Registry for Alzheimer's Disease (CERAD) [58]. A board-certified neuropathologist excluded cases with other pathologies (e.g., cerebral amyloid angiopathy, vascular dementia, dementia with Lewy bodies, hippocampal sclerosis, Parkinson's disease, and large strokes) and those treated with acetylcholinesterase inhibitors.

Cortical samples

Frontal cortex samples from Brodmann area 9, which contained the superior longitudinal WM tract, were immediately frozen at -80°C, cut into 20 µm thick sections onto gelatin-coated slides using a cryostat (Microm HM550, Walldorf, Germany) and stored at -25 °C prior autoradiography and MALDI-MSI assay. Functional autoradiography of M_2/M_4, CB_1 and $S1P_1$ receptors were performed using tissue from NCI, MCI, and AD. However, MALDI-MSI was performed in tissue obtained from the YAC, NCI, MCI, and AD groups.

MALDI-MSI

We used matrix-assisted laser desorption ionization as an imaging mass spectrometry method (MALDI – MSI) for the analysis of the lipid composition and anatomical distribution within FC GM and WM. Prior to the lipid analysis, sections from all cases, were sprayed (six passes) with cyano-4-hydroxycinnamic

acid (CHCA) as a chemical matrix at 10 mg/ml concentration in 50 % methanol using a Tissue MALDI sprayer (TM sprayer, HTX Technologies, LCC, Carrboro, NC, USA) with a flow rate of 120 ml/min and at 70ºC. We scanned the samples in both positive and negative ionization mode, in the range of m/z 500 – 1300 with a LTQ – Orbitrap – XL mass spectrometer (Thermo Fisher Scientific, San Jose), equipped with a nitrogen laser of λ = 337 nm, using a repetition rate = 60 Hz and a spot size= 80 × 120 µm. The scanned parameters were 2 µscans/step with 10 laser shots and a raster step size of 100 µm at laser fluency of 15 - 40 µJ.

The area scanned in each group included all cortical layers and WM (Fig. 1 A-D, region outlined by black box). For statistical analysis, lipid intensities in the white and gray matter delimited by red circles (Fig. 1 A-D) were exported separately in positive and negative ions using MSiReader software [59], as the average of absolute intensity in arbitrary units from each area and ionization mode. In addition, we exported the intensities from 5 lipid islands and 5 areas not containing similar accumulation within the GM in the positive ion mode. Lipid assignment was performed based on the m/z values with a 5-ppm mass accuracy as the tolerance window [60] using Lipid Maps (www.lipidmaps.org) or the Human metabolome Database (www.hmdb.ca) [59, 61] and reported previously [62-66]. For illustrative purposes, a section from each group was first scanned and then counterstained with thionine to aid in cytoarchitectonic determination [60] (see Fig. 1).

Functional autoradiography of activated $G\alpha_{i/o}$ proteins using a [^{35}S] GTPγS binding assay

Frozen sections from each case were dried, followed by two consecutive incubations in HEPES-based buffer (50 mM HEPES, 100 mM NaCl, 3 mM $MgCl_2$, 0.2 mM EGTA and 1% BSA, pH 7.4) for 30 min at 30°C to remove endogenous ligands. Briefly, sections were incubated for 2 h at 30°C in the same buffer

supplemented with 2 mM GDP, 1 mM DTT (Sigma, St. Louis, MO, USA) and 0.04 nM [^{35}S] GTPγS (initial specific activity 1250 Ci/mmol, Perkin Elmer, Boston, MA, USA). Basal binding was determined in two consecutive sections in the absence of the agonist. Agonist-stimulated binding using the same reaction buffer was determined in a consecutive cut section in the presence of the corresponding receptor agonists, WIN55,212-2 (10 μM) for CB_1 receptors, carbachol (100 μM) for M_2/M_4 receptors and CYM-5442 (10 μM) for $S1P_1$ receptors (Sigma-Aldrich, St. Louis, MO, USA). Non-specific binding was defined by competition with GTPγS (10 μM) in a consecutively cut section. Sections were then washed twice in cold (4°C) 50 mM HEPES buffer (pH 7.4), dried and exposed to β-radiation sensitive film (Kodak Biomax MR, Sigma. St. Louis, MO, USA) together with a set of [^{14}C] standards calibrated for ^{35}S [17].

Statistical analysis

The Kruskal-Wallis test was used to assess between-group comparisons on demographic, cognitive, lipidomic variables and autoradiographic data for NCI, MCI, and AD cases. The Dunn's test was used to identify statistically significant groupwise comparisons. Since a formal adjustment for multiple comparisons was not applied to the lipidomic variables, we used a nominal significance level of alpha = 0.01 to balance a Type I error rate with the need to identify associations with possible biological relevance. The total number of lipids analyzed in each area of the FC in both positive and negative ionization mode were white matter positive, n = 393; white matter negative, n = 69; gray matter positive, n = 588; gray matter negative, n = 169. The five lipids that exhibited changes in FC WM in NCI, MCI, and AD cases, were compared between the YAC and NCI groups using a Mann-Whitney test with a significance level set at p = 0.05. Analysis comparing areas with lipid accumulation *versus* those without accumulation in all RROS cases was performed using a Mann-Whitney test with a nominal significance level of alpha =

0.01. This analysis revealed a reduced number of significantly different lipids (see supplementary Fig. 1). We conducted groupwise comparisons across clinical groups using a Kruskal-Wallis test followed by Dun's test, with the p-value set at 0.05. Spearman correlation assessed data associations and significance was set to 0.01 to account for multiple comparisons, while still allowing for an adequate number of associations to be deemed significant. Statistical analysis was conducted using R 4.2.3. Data was graphically represented using GraphPad Prism 9 (GraphPad Software, San Diego, CA, USA).

RESULTS

Subject Characteristics

The demographic, clinical, and neuropathological characteristics of the 15 Rush Religious Orders Study (RROS) participants used in this study were summarized in Table 1. There were no significant differences in age, sex, years of education, *postmortem* interval (PMI), brain weight, semantic memory, working memory, visuospatial speed z-score, or possession of at least one apolipoprotein (ApoE) ε4 allele across groups the RROS cases. Mini-Mental State Examination (MMSE) scores were significantly lower in the AD compared to the NCI and MCI groups. Global cognition, episodic memory and perceptual speed score were lower in AD compared to NCI. The YAC subjects were significantly younger than the RROS NCI cases (68.83 ± 7.9 *vs* 86.27 ± 4.8 years, respectively; Mann-Whitney test; $p = 0.004$). Although a similar clinical evaluation was not available for the YAC cases, a review of their medical records did not reveal evidence of cognitive difficulties or neurological disease. Moreover, all cases in the YAC subjects had a *postmortem* neuropathological Braak score of 0, while the NCI cases displayed an average Braak score of 3.2 ± 0.8 (see Table 1). A Braak score of 0 has been used to select control cases for analysis in clinical pathological studies [67].

Frontal cortex MALDI-MSI analysis in NCI, MCI and AD

We conducted MALDI-MSI analysis on frozen FC tissue obtained from elderly participants of the RROS that died with a clinical diagnosis of NCI, MCI, and AD and YAC cases with no cognitive impairment from the University of the Basque Country to identify phospholipids and sphingolipids by measuring the charged lipids in both positive and negative ions. Significant lipid changes were found only in the WM between clinical groups. The relative intensity levels of diacylglycerol (DG) 36:2 (Fig. 1 E-H, Fig. 2 A, $p<0.05$), DG 38:5 (Fig. 1 I-L, Fig. 2 B, $p<0.05$), and phosphatidic acid (PA) 40:6 (Fig. 1 M-P, Fig. 2 C, $p<0.05$) were significantly higher in MCI compared to elderly NCI cases, while phosphatidylinositol (PI) 38:5 (Fig. 1 Q-T, Fig. 2 D, $p<0.05$) and PI 38:4 (Fig. 1 U-X, Fig. 2 E, $p<0.01$) were lower in AD compared to NCI subjects. DG 36:2, DG 38:5, and PA 40:6 intensities were greater in WM compared to GM (Fig. 1 E-P), while PI 38:5 and PI 38:4, were more intense in GM than WM (Fig. 1 Q-X) in all experimental groups.

In addition, we also assessed the effect of differences in age between the NCI and YAC cases had upon FC lipid intensity. Here we found lower intensity levels of DG 36:2 (Fig. 1 E-F, Fig. 2 F, $p<0.01$), DG 38:5 (Fig. 1 I-J, Fig. 2 G, $p<0.01$), PA 40:6 (Fig. 1 M-N, Fig. 2 H, $p<0.01$), PI 38:5 (Fig. 1 Q-R, Fig. 2 I, $p<0.05$), and PI 38:4 (Fig. 1 U-V, Fig. 2 J, $p<0.05$) in YAC compared to NCI subjects.

Frontal cortex lipid accumulations in GM in NCI, MCI and AD

There was no difference in lipid composition in the GM across the groups. However, MALDI image analysis revealed discrete lipid patches in the supragranular layers of the GM (Supplementary Fig. S1), which displayed increased lipid intensity (%) for several phosphatidylcholines (PC) (PC 30:0, PC 32:0, PC 34:0, PC 32:1, PC 36:4, and PC 38:4) diacylglycerols (DG) (DG 30:0, DG 32:0, PC 34:0, DG

32:1, DG 34:3, DG 36:3, and DG 38:4), phosphatidic acids (PA) (PA 36:5, PA 36:4, PA 40:5, and PA 34:4) sphingomyelins (SM) (SM 36:1 and SM 38:1), ceramides (CER) (CER 36:1) and phosphatidylethanolamines (PE) (PE 40:7 and PE 44:12) and a downregulation of PA 36:2 and SM 42:2 compared to areas lacking these patches across all clinical groups (Supplementary Fig. S1). Conversely, only three lipids were increased between clinical groups. Specifically, PC 32:1 (Fig. 3 A-C, J, $p<0.05$) and SM 38:1 (Fig. 3 G-I, L, $p<0.05$) showed greater intensity in AD compared to NCI, while PC 34:0 (Fig. 3 D-F K, $p<0.05$) exhibited a significant elevation in MCI compared to NCI.

Frontal cortex functional autoradiography of activated $G\alpha_{i/o}$ proteins by the [^{35}S]GTPγS binding assay in NCI, MCI and AD cases

Functional coupling induced by carbachol for M_2/M_4-mediated receptor activity, was decreased in the FC GM in AD, specifically in layer V-VI compared to MCI. Additionally, [^{35}S]GTPγS binding induced by WIN55,212-2, primarily mediated by CB_1 activity, was increased in FC layer V-VI in AD compared to NCI. Lastly, functional coupling of $S1P_1$ receptors to $G_{i/o}$ proteins, induced by the specific agonist CYM5442, was reduced in FC WM in AD compared to NCI (Fig. 4 and Table 2).

Associations between lipids, receptor activity and demographic variables

A significant positive correlation was observed between PI 38:5 and perceptual speed (Fig. 5 A, $r = 0.66$, $p = 0.009$), while phosphatidylethanolamine (PE) 42:9 (Fig. 5 C, $r = -0.75$, $p = 0.002$) and PE 42:10 (Fig. 5 C, $r = -0.7$, $p = 0.004$) GM intensity levels negatively correlated with perceptual speed z-score values across clinical groups. PE 42:9 in GM correlated negatively with MMSE scores (Fig. 4 E, $r = -0.89$, $p<0.0001$). In addition, we found a positive correlation between the lipid intensity of the discrete oval accumulations of PC 32:1 and CB_1 stimulation in GM layers V-VI (Fig. 5 H, $r = 0.83$, $p=0.0002$). A negative correlation was found between PC 32:1 and perceptual speed across clinical groups (Fig. 5 B,

$r = -0.62$, $p = 0.016$). A negative correlation was found between sphingomyelin (SM) 38:1 (Fig. 5 F, $r = -0.74$, $p=0.002$) and MMSE across groups.

DISCUSSION

While multiple studies have demonstrated lipid alterations in the AD brain, the involvement of neurolipids together with their lipid precursors remain under-investigated during the progression of AD [68]. Here we showed significant lipid alterations in the WM in MCI, suggesting an early role in the onset of AD. Specifically, we found an increase in phosphatidic acid (PA) 40:6 and diacylglycerol (DG) 36:2 and DG 38:5 in MCI compared to NCI, and a decrease of phosphatidylinositol (PI) 38:5 and PI 38:4 in AD compared to NCI. The intensity of DGs and PA were higher in the WM compared to GM. Regarding the metabolic origins of DG and PA, phospholipid degradation emerges as a significant lipidomic pathway. PA and DG are important membrane lipids and second messengers that contribute to cellular processes either by their biophysical effect directly on the cell membrane or by recruiting proteins to the membrane [69]. The main pathway that regulates the formation and levels of these lipids is the phosphorylation of PI and activation of phospholipase C (PLC) to generate DG, which remains associated with the plasma membrane and generates PA [70]. Although numerous studies have documented the elevation of DGs in MCI [9, 71, 72], we found an increase within the WM in this prodromal stage suggesting that DGs are early indicators of WM damage. However, the precise mechanism(s) underlying the heightened levels of DG in the FC WM in MCI require further investigation. Additionally, we demonstrated decreased activity of M_2/M_4 receptors, stimulated by Carbachol, in layers V-VI in AD compared to MCI. Previous studies have shown a reduction in the density of total muscarinic receptors in cortical areas in AD [73]. In particular, pre-synaptic M_2 receptor density and G-protein coupling of this receptor was decreased in AD cortex [74, 75], supporting the current reduction of cortical muscarinic receptor activity in AD. In contrast, we found a non-significant trend for an increase in M_2/M_4 activity in

MCI compared to NCI. Interestingly, muscarinic receptors are known to mediate lipid signaling via the neurotransmitter ACh, which activates phospholipases to generate DG in synaptosomes both in *in vivo* and *in vitro* [76-78]. However, lipid signaling can be initiated through diverse pathways and receptors including cholinergic and non-cholinergic receptors [27-29] that modify phospholipases resulting in a localized accumulation of PA and DG. Accumulations of these lipid have been reported to modify the recruitment of proteins and fission processes related to WM membrane stability, which is detrimental to the maintenance of axonal connectivity [79, 80], results in a negative curvature to membrane bilayers due to their conical shape [81]. Perhaps increased levels of DG and PA are early indicators of WM dysfunction that, in part, underlie the cognitive deficits seen in prodromal AD.

Whether lipid modifications are associated with the onset of deficits in cognitive performance in AD is an under investigated area. In this regard, we found a downregulation of WM PI 38:5/38:4, which corresponds to arachidonic acid-enriched phosphatidylinositol (PI-AAs) (PI 18:0_20:4 and PI 18:1_20:4) [62, 63] in AD compared to NCI that correlated with impaired perceptual speed performance across groups. Evaluation of PI (18:0_20:4) images revealed more intense labeling in GM than WM. It has been reported that PIP_2 (18:0_20:4), resulting from the degradation of the PI-AA (18:0_20:4), was greater in WM myelin-enriched fractions [82] supporting the suggestion that alterations in phosphoinositide's and their respective regulatory pathways, play a role in WM and axon signaling dysfunction [83]. Another crucial regulatory pathway for PI (18:0_20:4) involves phospholipase A_2 (PLA_2), which maintains a balance between the conversion of arachidonic acid (AA) into proinflammatory mediators and reincorporation into PI-AA [84, 85]. AA, a key mediator of neuroinflammation, is elevated in AD and predominantly accumulates in the outer membrane of neurons and the myelin sheath [86] suggesting that the integrity of myelinated axons is compromised early in AD. Damage to the WM, which is comprised of 80% lipids, may disrupt neural transmission resulting in sensory, motor, and cognitive impairments

[86]. These findings are consistent with studies demonstrating disruption of WM in prodromal AD [87, 88]. We observed that the WM displayed a reduction of $S1P_1$ receptor activity, while CB_1 receptor activity within the infragranular layers of the grey matter which also contains heavily myelinated fibers [89, 90] are increased in AD compared to NCI. An imbalance between CB_1 and $S1P_1$ has been suggested to play a role in the maintenance of myelin integrity in AD [91, 92]. In this regard, alterations in the activity of these receptors may be attributed to changes in their endogenous agonists. For example, levels of the $S1P_1$ receptor agonist sphingosine 1 phosphate (S1P) are decreased in cortical grey and WM in early and advanced AD [93, 94], while signaling for the 2-arachidonoylglycerol (2-AG) an endocannabinoid endogenous CB_1 receptor agonist increases in response to Aβ plaques [95]. Both, CB_1 And $S1P_1$ receptor activity, negatively correlated while the temporal relationship or signaling crosstalk between these receptors remain unknown [96]. However, activation of CB_1 receptors drives the breakdown of sphingomyelin into ceramide, followed by its conversion to sphingosine. Subsequently, sphingosine is phosphorylated by sphingosine kinases to generate S1P, which binds to $S1P_1$ receptors [97, 98] suggesting that CB_1 receptors activate $S1P_1$ pathways in response to WM dysfunction.

Here, we also demonstrated that PA 40:6, DG 36:2, DG 38:5 and PI-AAs, which play a key role in WM myelination and maintenance, were significatively increased in older NCI compared to younger YAC subjects. Since myelinated axons in WM deteriorate structurally and functionally with age and are associated with poorer cognitive ability [99-102], an increase in PA 40:6, DG 36:2, DG 38:5 and PI-AA in NCI, suggests that normal physiological aging affects axonal and myelin lipids metabolism in the FC [103]. Although, we do not rule out the possibility that differences in ethnicity and lifestyle (i.e., diet and exercise) between YAC and NCI may influence the observed lipid changes with age in the WM [104], further investigation is needed to evaluate these lipid changes.

In the supragranular layers of the FC, patches of lipid displayed a significant increase in the intensity of PC 32:1, PC 34:0 and SM 38:1. Interestingly, PC 34:0 containing aggregates were seen in MCI, while both SM 38:1 and PC 32:1 were increased in AD. However, only the latter two lipids correlated with cognitive decline in AD. Each of these lipids are found in activated microglia [105], gliomas [106] and Aβ plaques in human and animal models of AD [14, 107-110]. Perhaps the upregulation of PC 32:1, PC 34:0 and SM 38:1 plays a key role in the pathogenesis of AD.

It is important to discuss limitations associated with the current study. For example, the small number of cases warrant a conservative interpretation of the findings requiring validation in a larger cohort, which would allow for correlations with ApoE genotypes, a major risk factor for the onset of AD and its neuropathologic lesions. It should be noted that the RROS participants were from a community-based population of highly educated retired clergy who had excellent health care and nutrition and were used in multiple clinical pathological [111, 112] and epidemiological investigations [41] of AD. However, other findings reported using tissue from the RROS cohort have not been found to be different from those derived from non-clerical populations [113, 114]. Individuals who volunteer may introduce bias by decreasing pathology, but this is partially overcome by the RROS high follow-up and autopsy rates [115]. Another caveat is that the YAC cases lacked a detailed pre-clinical evaluation. However, there was no evidence of impairment in cognition or adverse neurological disease documented in their medical records. On the other hand, all YAC cases were neuropathologically classified as Braak stage 0, indicative of no cognitive impairment [56]. "The possibility exists that differences in ethnicity and lifestyle (i.e., diet and exercise) may have influenced the observed difference in lipid values found between the YAC and NCI cases in the WM [103]. The influence that these cultural variables have upon lipid expression requires further investigation."

Strengths of this study include uniform *premortem* clinical and *postmortem* pathological evaluation and that final the pathologic classification was performed without knowledge of the clinical evaluation for the RROS cases.

In summary, the present findings provide evidence that lipidomic dysfunction is associated with the cognitive impairment seen in the prodromal phase of AD. The current findings indicate that modifications in WM myelin-related lipids and cholinergic receptors play a pivotal role in the onset of AD dementia and potentially serve as novel drug targets.

ACKNOWLEDGMENTS

We are indebted to the nuns, priests, and lay brothers who participated in the Rush Religious Orders Study and to the members of the Rush ADC. Technical and human support provided by University of the Basque Country (UPV/EHU), Ministry of Economy and Competitiveness (MINECO), Basque Government (GV/EJ), European Regional Development Fund (ERDF), and European Social Fund (ESF) and the collaboration of Ivan Fernandez is gratefully acknowledged. J.M.-G. is the recipient of "Margarita Salas" fellowship.

FUNDING

This study was supported by grants PO1AG014449, RO1AG043375, P30AG010161 and P30AG042146, RF1AG081286 from the National Institute on Aging, Barrow Neurological Institute and Arizona Alzheimer's Consortium. This work also was supported by grants from the regional Basque Government IT1454-22 to the "Neurochemistry and Neurodegeneration" consolidated research group and by Instituto

de Salud Carlos III through the project "PI20/00153" (co-funded by European Regional Development Fund "A way to make Europe") and by BIOEF project BIO22/ALZ/010 funded by Eitb Maratoia.

CONFLICT OF INTEREST

The authors declare no competing interests.

DATA AVALILABILITY

The data supporting the findings of this study are available within the article and in the supplementary material.

REFERENCES

[1] Yin F (2023) Lipid metabolism and Alzheimer's disease: clinical evidence, mechanistic link and therapeutic promise. *FEBS J* **290**, 1420-1453.

[2] Fabelo N, Martin V, Marin R, Moreno D, Ferrer I, Diaz M (2014) Altered lipid composition in cortical lipid rafts occurs at early stages of sporadic Alzheimer's disease and facilitates APP/BACE1 interactions. *Neurobiol Aging* **35**, 1801-1812.

[3] Prasad MR, Lovell MA, Yatin M, Dhillon H, Markesbery WR (1998) Regional membrane phospholipid alterations in Alzheimer's disease. *Neurochem Res* **23**, 81-88.

[4] Nitsch RM, Blusztajn JK, Pittas AG, Slack BE, Growdon JH, Wurtman RJ (1992) Evidence for a membrane defect in Alzheimer disease brain. *Proc Natl Acad Sci U S A* **89**, 1671-1675.

[5] Stokes CE, Hawthorne JN (1987) Reduced phosphoinositide concentrations in anterior temporal cortex of Alzheimer-diseased brains. *J Neurochem* **48**, 1018-1021.

[6] Han X, D MH, McKeel DW, Jr., Kelley J, Morris JC (2002) Substantial sulfatide deficiency and ceramide elevation in very early Alzheimer's disease: potential role in disease pathogenesis. *J Neurochem* **82**, 809-818.

[7] Soderberg M, Edlund C, Alafuzoff I, Kristensson K, Dallner G (1992) Lipid composition in different regions of the brain in Alzheimer's disease/senile dementia of Alzheimer's type. *J Neurochem* **59**, 1646-1653.

[8] Cheng H, Wang M, Li JL, Cairns NJ, Han X (2013) Specific changes of sulfatide levels in individuals with pre-clinical Alzheimer's disease: an early event in disease pathogenesis. *J Neurochem* **127**, 733-738.

[9] Wood PL, Medicherla S, Sheikh N, Terry B, Phillipps A, Kaye JA, Quinn JF, Woltjer RL (2015) Targeted Lipidomics of Fontal Cortex and Plasma Diacylglycerols (DAG) in Mild Cognitive Impairment and Alzheimer's Disease: Validation of DAG Accumulation Early in the Pathophysiology of Alzheimer's Disease. *J Alzheimers Dis* **48**, 537-546.

[10] Couttas TA, Kain N, Suchowerska AK, Quek LE, Turner N, Fath T, Garner B, Don AS (2016) Loss of ceramide synthase 2 activity, necessary for myelin biosynthesis, precedes tau pathology in the cortical pathogenesis of Alzheimer's disease. *Neurobiol Aging* **43**, 89-100.

[11] Hu H, Laskin J (2022) Emerging Computational Methods in Mass Spectrometry Imaging. *Adv Sci (Weinh)* **9**, e2203339.

[12] Schubert KO, Weiland F, Baune BT, Hoffmann P (2016) The use of MALDI-MSI in the investigation of psychiatric and neurodegenerative disorders: A review. *Proteomics* **16**, 1747-1758.

[13] Martinez-Gardeazabal J, Gonzalez de San Roman E, Moreno-Rodriguez M, Llorente-Ovejero A, Manuel I, Rodriguez-Puertas R (2017) Lipid mapping of the rat brain for models of disease. *Biochim Biophys Acta Biomembr* **1859**, 1548-1557.

[14] Wehrli PM, Ge J, Michno W, Koutarapu S, Dreos A, Jha D, Zetterberg H, Blennow K, Hanrieder J (2023) Correlative Chemical Imaging and Spatial Chemometrics Delineate Alzheimer Plaque Heterogeneity at High Spatial Resolution. *JACS Au* **3**, 762-774.

[15] Kaya I, Jennische E, Dunevall J, Lange S, Ewing AG, Malmberg P, Baykal AT, Fletcher JS (2020) Spatial Lipidomics Reveals Region and Long Chain Base Specific Accumulations of Monosialogangliosides in Amyloid Plaques in Familial Alzheimer's Disease Mice (5xFAD) Brain. *ACS Chem Neurosci* **11**, 14-24.

[16] Zhang Q, Li Y, Sui P, Sun XH, Gao Y, Wang CY (2023) MALDI mass spectrometry imaging discloses the decline of sulfoglycosphingolipid and glycerophosphoinositol species in the brain regions related to cognition in a mouse model of Alzheimer's disease. *Talanta* **266**, 125022.

[17] Gonzalez de San Roman E, Llorente-Ovejero A, Martinez-Gardeazabal J, Moreno-Rodriguez M, Gimenez-Llort L, Manuel I, Rodriguez-Puertas R (2021) Modulation of Neurolipid Signaling and Specific Lipid Species in the Triple Transgenic Mouse Model of Alzheimer's Disease. *Int J Mol Sci* **22**.

[18] Llorente-Ovejero A, Martinez-Gardeazabal J, Moreno-Rodriguez M, Lombardero L, Gonzalez de San Roman E, Manuel I, Giralt MT, Rodriguez-Puertas R (2021) Specific Phospholipid Modulation by Muscarinic Signaling in a Rat Lesion Model of Alzheimer's Disease. *ACS Chem Neurosci* **12**, 2167-2181.

[19] Gonzalez de San Roman E, Manuel I, Giralt MT, Ferrer I, Rodriguez-Puertas R (2017) Imaging mass spectrometry (IMS) of cortical lipids from preclinical to severe stages of Alzheimer's disease. *Biochim Biophys Acta Biomembr* **1859**, 1604-1614.

[20] Yuki D, Sugiura Y, Zaima N, Akatsu H, Takei S, Yao I, Maesako M, Kinoshita A, Yamamoto T, Kon R, Sugiyama K, Setou M (2014) DHA-PC and PSD-95 decrease after loss of synaptophysin and before neuronal loss in patients with Alzheimer's disease. *Sci Rep* **4**, 7130.

[21] Grimm MO, Grosgen S, Riemenschneider M, Tanila H, Grimm HS, Hartmann T (2011) From brain to food: analysis of phosphatidylcholins, lyso-phosphatidylcholins and phosphatidylcholin-plasmalogens derivates in Alzheimer's disease human post mortem brains and mice model via mass spectrometry. *J Chromatogr A* **1218**, 7713-7722.

[22] Buckner RL, Andrews-Hanna JR, Schacter DL (2008) The brain's default network: anatomy, function, and relevance to disease. *Ann N Y Acad Sci* **1124**, 1-38.

[23] Mesulam MM (2013) Cholinergic circuitry of the human nucleus basalis and its fate in Alzheimer's disease. *J Comp Neurol* **521**, 4124-4144.

[24] Kao YC, Ho PC, Tu YK, Jou IM, Tsai KJ (2020) Lipids and Alzheimer's Disease. *Int J Mol Sci* **21**.

[25] Vance JE, Campenot RB, Vance DE (2000) The synthesis and transport of lipids for axonal growth and nerve regeneration. *Biochim Biophys Acta* **1486**, 84-96.

[26] Wurtman RJ (1992) Choline metabolism as a basis for the selective vulnerability of cholinergic neurons. *Trends Neurosci* **15**, 117-122.

[27] Selley DE, Welch SP, Sim-Selley LJ (2013) Sphingosine lysolipids in the CNS: endogenous cannabinoid antagonists or a parallel pain modulatory system? *Life Sci* **93**, 187-193.

[28] Hla T (2004) Physiological and pathological actions of sphingosine 1-phosphate. *Semin Cell Dev Biol* **15**, 513-520.

[29] Di Marzo V, Bisogno T, De Petrocellis L, Melck D, Martin BR (1999) Cannabimimetic fatty acid derivatives: the anandamide family and other endocannabinoids. *Curr Med Chem* **6**, 721-744.

[30] Llorente-Ovejero A, Manuel I, Giralt MT, Rodriguez-Puertas R (2017) Increase in cortical endocannabinoid signaling in a rat model of basal forebrain cholinergic dysfunction. *Neuroscience* **362**, 206-218.
[31] Gessa GL, Casu MA, Carta G, Mascia MS (1998) Cannabinoids decrease acetylcholine release in the medial-prefrontal cortex and hippocampus, reversal by SR 141716A. *Eur J Pharmacol* **355**, 119-124.
[32] Garzon M, Chan J, Mackie K, Pickel VM (2022) Prefrontal cortical distribution of muscarinic M2 and cannabinoid-1 (CB1) receptors in adult male mice with or without chronic adolescent exposure to Delta9-tetrahydrocannabinol. *Cereb Cortex* **32**, 5420-5437.
[33] Garzon M, Wang G, Chan J, Bourie F, Mackie K, Pickel VM (2021) Adolescent administration of Delta(9)-THC decreases the expression and function of muscarinic-1 receptors in prelimbic prefrontal cortical neurons of adult male mice. *IBRO Neurosci Rep* **11**, 144-155.
[34] Fernandez-Moncada I, Eraso-Pichot A, Dalla Tor T, Fortunato-Marsol B, Marsicano G (2023) An enquiry to the role of CB1 receptors in neurodegeneration. *Neurobiol Dis* **184**, 106235.
[35] Estrada JA, Contreras I (2020) Endocannabinoid Receptors in the CNS: Potential Drug Targets for the Prevention and Treatment of Neurologic and Psychiatric Disorders. *Curr Neuropharmacol* **18**, 769-787.
[36] Manuel I, Gonzalez de San Roman E, Giralt MT, Ferrer I, Rodriguez-Puertas R (2014) Type-1 cannabinoid receptor activity during Alzheimer's disease progression. *J Alzheimers Dis* **42**, 761-766.
[37] Ramirez BG, Blazquez C, Gomez del Pulgar T, Guzman M, de Ceballos ML (2005) Prevention of Alzheimer's disease pathology by cannabinoids: neuroprotection mediated by blockade of microglial activation. *J Neurosci* **25**, 1904-1913.
[38] Ahmad R, Goffin K, Van den Stock J, De Winter FL, Cleeren E, Bormans G, Tournoy J, Persoons P, Van Laere K, Vandenbulcke M (2014) In vivo type 1 cannabinoid receptor availability in Alzheimer's disease. *Eur Neuropsychopharmacol* **24**, 242-250.
[39] Ceccom J, Loukh N, Lauwers-Cances V, Touriol C, Nicaise Y, Gentil C, Uro-Coste E, Pitson S, Maurage CA, Duyckaerts C, Cuvillier O, Delisle MB (2014) Reduced sphingosine kinase-1 and enhanced sphingosine 1-phosphate lyase expression demonstrate deregulated sphingosine 1-phosphate signaling in Alzheimer's disease. *Acta Neuropathol Commun* **2**, 12.
[40] Schmitt FA, Nelson PT, Abner E, Scheff S, Jicha GA, Smith C, Cooper G, Mendiondo M, Danner DD, Van Eldik LJ, Caban-Holt A, Lovell MA, Kryscio RJ (2012) University of Kentucky Sanders-Brown healthy brain aging volunteers: donor characteristics, procedures and neuropathology. *Curr Alzheimer Res* **9**, 724-733.
[41] Mufson EJ, Chen EY, Cochran EJ, Beckett LA, Bennett DA, Kordower JH (1999) Entorhinal cortex beta-amyloid load in individuals with mild cognitive impairment. *Exp Neurol* **158**, 469-490.
[42] Folstein MF, Folstein SE, McHugh PR (1975) "Mini-mental state". A practical method for grading the cognitive state of patients for the clinician. *J Psychiatr Res* **12**, 189-198.
[43] Morris JC, Heyman A, Mohs RC, Hughes JP, van Belle G, Fillenbaum G, Mellits ED, Clark C (1989) The Consortium to Establish a Registry for Alzheimer's Disease (CERAD). Part I. Clinical and neuropsychological assessment of Alzheimer's disease. *Neurology* **39**, 1159-1165.
[44] SMITH A (1984) Symbol Digit Modalities Test manual-R. *Western Psychological, Los Angeles.*
[45] WECHSLER D (1987) Wechsler Memory Scale-Revised Manual. *Psychological Corporation, New York.*
[46] GOODGLASS H (1972) Kaplan. Assessment of aphasia and related disorders. *Lea & Febiger, Philadelphia*.
[47] Benton AL, Varney NR, Hamsher KD (1978) Visuospatial judgment. A clinical test. *Arch Neurol* **35**, 364-367.
[48] RAVEN. J.C. JHC, AND J. RAVEN (1992) Standard progressive matrices-1992 edition; Raven manual: Section 3. *Oxford Psychologists Press, Oxford*.
[49] Pittman J, Andrews H, Tatemichi T, Link B, Struening E, Stern Y, Mayeux R (1992) Diagnosis of dementia in a heterogeneous population. A comparison of paradigm-based diagnosis and physician's diagnosis. *Arch Neurol* **49**, 461-467.
[50] Stern Y, Gurland B, Tatemichi TK, Tang MX, Wilder D, Mayeux R (1994) Influence of education and occupation on the incidence of Alzheimer's disease. *JAMA* **271**, 1004-1010.

[51] McKhann G, Drachman D, Folstein M, Katzman R, Price D, Stadlan EM (1984) Clinical diagnosis of Alzheimer's disease: report of the NINCDS-ADRDA Work Group under the auspices of Department of Health and Human Services Task Force on Alzheimer's Disease. *Neurology* **34**, 939-944.
[52] Devanand DP, Folz M, Gorlyn M, Moeller JR, Stern Y (1997) Questionable dementia: clinical course and predictors of outcome. *J Am Geriatr Soc* **45**, 321-328.
[53] Ebly EM, Hogan DB, Parhad IM (1995) Cognitive impairment in the nondemented elderly. Results from the Canadian Study of Health and Aging. *Arch Neurol* **52**, 612-619.
[54] Petersen RC, Smith GE, Ivnik RJ, Tangalos EG, Schaid DJ, Thibodeau SN, Kokmen E, Waring SC, Kurland LT (1995) Apolipoprotein E status as a predictor of the development of Alzheimer's disease in memory-impaired individuals. *JAMA* **273**, 1274-1278.
[55] Perez SE, Getova DP, He B, Counts SE, Geula C, Desire L, Coutadeur S, Peillon H, Ginsberg SD, Mufson EJ (2012) Rac1b increases with progressive tau pathology within cholinergic nucleus basalis neurons in Alzheimer's disease. *Am J Pathol* **180**, 526-540.
[56] Braak H, Braak E (1991) Neuropathological stageing of Alzheimer-related changes. *Acta Neuropathol* **82**, 239-259.
[57] Newell KL, Hyman BT, Growdon JH, Hedley-Whyte ET (1999) Application of the National Institute on Aging (NIA)-Reagan Institute criteria for the neuropathological diagnosis of Alzheimer disease. *J Neuropathol Exp Neurol* **58**, 1147-1155.
[58] Mirra SS (1997) The CERAD neuropathology protocol and consensus recommendations for the postmortem diagnosis of Alzheimer's disease: a commentary. *Neurobiol Aging* **18**, S91-94.
[59] Robichaud G, Garrard KP, Barry JA, Muddiman DC (2013) MSiReader: an open-source interface to view and analyze high resolving power MS imaging files on Matlab platform. *J Am Soc Mass Spectrom* **24**, 718-721.
[60] Martinez-Gardeazabal J, Moreno-Rodriguez M, de San Roman EG, Abad B, Manuel I, Rodriguez-Puertas R (2023) Mass Spectrometry for the Advancement of Lipid Analysis in Alzheimer's Research. *Methods Mol Biol* **2561**, 245-259.
[61] Wishart DS, Feunang YD, Marcu A, Guo AC, Liang K, Vazquez-Fresno R, Sajed T, Johnson D, Li C, Karu N, Sayeeda Z, Lo E, Assempour N, Berjanskii M, Singhal S, Arndt D, Liang Y, Badran H, Grant J, Serra-Cayuela A, Liu Y, Mandal R, Neveu V, Pon A, Knox C, Wilson M, Manach C, Scalbert A (2018) HMDB 4.0: the human metabolome database for 2018. *Nucleic Acids Res* **46**, D608-D617.
[62] Angerer TB, Bour J, Biagi JL, Moskovets E, Frache G (2022) Evaluation of 6 MALDI-Matrices for 10 mum Lipid Imaging and On-Tissue MSn with AP-MALDI-Orbitrap. *J Am Soc Mass Spectrom* **33**, 760-771.
[63] Cheng H, Sun G, Yang K, Gross RW, Han X (2010) Selective desorption/ionization of sulfatides by MALDI-MS facilitated using 9-aminoacridine as matrix. *J Lipid Res* **51**, 1599-1609.
[64] Seyer A, Cantiello M, Bertrand-Michel J, Roques V, Nauze M, Bezirard V, Collet X, Touboul D, Brunelle A, Comera C (2013) Lipidomic and spatio-temporal imaging of fat by mass spectrometry in mice duodenum during lipid digestion. *PLoS One* **8**, e58224.
[65] Liu Y, Chen L, Qin L, Han M, Li J, Luo F, Xue K, Feng J, Zhou Y, Wang X (2019) Enhanced in situ detection and imaging of lipids in biological tissues by using 2,3-dicyanohydroquinone as a novel matrix for positive-ion MALDI-MS imaging. *Chem Commun (Camb)* **55**, 12559-12562.
[66] Fort PE, Rajendiran TM, Soni T, Byun J, Shan Y, Looker HC, Nelson RG, Kretzler M, Michailidis G, Roger JE, Gardner TW, Abcouwer SF, Pennathur S, Afshinnia F (2021) Diminished retinal complex lipid synthesis and impaired fatty acid beta-oxidation associated with human diabetic retinopathy. *JCI Insight* **6**.
[67] Mufson EJ, Malek-Ahmadi M, Perez SE, Chen K (2016) Braak staging, plaque pathology, and APOE status in elderly persons without cognitive impairment. *Neurobiol Aging* **37**, 147-153.
[68] Di Paolo G, Kim TW (2011) Linking lipids to Alzheimer's disease: cholesterol and beyond. *Nat Rev Neurosci* **12**, 284-296.
[69] Qian Z, Drewes LR (1991) Cross-talk between receptor-regulated phospholipase D and phospholipase C in brain. *FASEB J* **5**, 315-319.

[70] De Craene JO, Bertazzi DL, Bar S, Friant S (2017) Phosphoinositides, Major Actors in Membrane Trafficking and Lipid Signaling Pathways. *Int J Mol Sci* **18**.
[71] Kim SH, Yang JS, Lee JC, Lee JY, Lee JY, Kim E, Moon MH (2018) Lipidomic alterations in lipoproteins of patients with mild cognitive impairment and Alzheimer's disease by asymmetrical flow field-flow fractionation and nanoflow ultrahigh performance liquid chromatography-tandem mass spectrometry. *J Chromatogr A* **1568**, 91-100.
[72] Wood PL, Barnette BL, Kaye JA, Quinn JF, Woltjer RL (2015) Non-targeted lipidomics of CSF and frontal cortex grey and white matter in control, mild cognitive impairment, and Alzheimer's disease subjects. *Acta Neuropsychiatr* **27**, 270-278.
[73] Rodriguez-Puertas R, Pascual J, Vilaro T, Pazos A (1997) Autoradiographic distribution of M1, M2, M3, and M4 muscarinic receptor subtypes in Alzheimer's disease. *Synapse* **26**, 341-350.
[74] Mash DC, Flynn DD, Potter LT (1985) Loss of M2 muscarine receptors in the cerebral cortex in Alzheimer's disease and experimental cholinergic denervation. *Science* **228**, 1115-1117.
[75] Flynn DD, Ferrari-DiLeo G, Levey AI, Mash DC (1995) Differential alterations in muscarinic receptor subtypes in Alzheimer's disease: implications for cholinergic-based therapies. *Life Sci* **56**, 869-876.
[76] Willars GB, Nahorski SR, Challiss RA (1998) Differential regulation of muscarinic acetylcholine receptor-sensitive polyphosphoinositide pools and consequences for signaling in human neuroblastoma cells. *J Biol Chem* **273**, 5037-5046.
[77] Lyeth BG, Gong QZ, Dhillon HS, Prasad MR (1996) Effects of muscarinic receptor antagonism on the phosphatidylinositol bisphosphate signal transduction pathway after experimental brain injury. *Brain Res* **742**, 63-70.
[78] Schmidt M, Nehls C, Rumenapp U, Jakobs KH (1996) m3 Muscarinic receptor-induced and Gi-mediated heterologous potentiation of phospholipase C stimulation: role of phosphoinositide synthesis. *Mol Pharmacol* **50**, 1038-1046.
[79] Kooijman EE, Burger KN (2009) Biophysics and function of phosphatidic acid: a molecular perspective. *Biochim Biophys Acta* **1791**, 881-888.
[80] Goni FM, Alonso A (1999) Structure and functional properties of diacylglycerols in membranes. *Prog Lipid Res* **38**, 1-48.
[81] Ganesan S, Shabits BN, Zaremberg V (2015) Tracking Diacylglycerol and Phosphatidic Acid Pools in Budding Yeast. *Lipid Insights* **8**, 75-85.
[82] Pathmasiri KC, Pergande MR, Tobias F, Rebiai R, Rosenhouse-Dantsker A, Bongarzone ER, Cologna SM (2020) Mass spectrometry imaging and LC/MS reveal decreased cerebellar phosphoinositides in Niemann-Pick type C1-null mice. *J Lipid Res* **61**, 1004-1013.
[83] Eichberg J, Dawson RM (1965) Polyphosphoinositides in myelin. *Biochem J* **96**, 644-650.
[84] Hiraide T, Ikegami K, Sakaguchi T, Morita Y, Hayasaka T, Masaki N, Waki M, Sugiyama E, Shinriki S, Takeda M, Shibasaki Y, Miyazaki S, Kikuchi H, Okuyama H, Inoue M, Setou M, Konno H (2016) Accumulation of arachidonic acid-containing phosphatidylinositol at the outer edge of colorectal cancer. *Sci Rep* **6**, 29935.
[85] Lee HC, Inoue T, Imae R, Kono N, Shirae S, Matsuda S, Gengyo-Ando K, Mitani S, Arai H (2008) Caenorhabditis elegans mboa-7, a member of the MBOAT family, is required for selective incorporation of polyunsaturated fatty acids into phosphatidylinositol. *Mol Biol Cell* **19**, 1174-1184.
[86] Salem N, Jr., Wegher B, Mena P, Uauy R (1996) Arachidonic and docosahexaenoic acids are biosynthesized from their 18-carbon precursors in human infants. *Proc Natl Acad Sci U S A* **93**, 49-54.
[87] Zhang HQ, Chau ACM, Shea YF, Chiu PK, Bao YW, Cao P, Mak HK (2023) Disrupted Structural White Matter Network in Alzheimer's Disease Continuum, Vascular Dementia, and Mixed Dementia: A Diffusion Tensor Imaging Study. *J Alzheimers Dis* **94**, 1487-1502.
[88] Zhou Y, Wei L, Gao S, Wang J, Hu Z (2023) Characterization of diffusion magnetic resonance imaging revealing relationships between white matter disconnection and behavioral disturbances in mild cognitive impairment: a systematic review. *Front Neurosci* **17**, 1209378.

[89] Chang S, Varadarajan D, Yang J, Chen IA, Kura S, Magnain C, Augustinack JC, Fischl B, Greve DN, Boas DA, Wang H (2022) Scalable mapping of myelin and neuron density in the human brain with micrometer resolution. *Sci Rep* **12**, 363.

[90] Tan SS, Kalloniatis M, Truong HT, Binder MD, Cate HS, Kilpatrick TJ, Hammond VE (2009) Oligodendrocyte positioning in cerebral cortex is independent of projection neuron layering. *Glia* **57**, 1024-1030.

[91] Song H, McEwen HP, Duncan T, Lee JY, Teo JD, Don AS (2021) Sphingosine kinase 2 is essential for remyelination following cuprizone intoxication. *Glia* **69**, 2863-2881.

[92] Tomas-Roig J, Agbemenyah HY, Celarain N, Quintana E, Ramio-Torrenta L, Havemann-Reinecke U (2020) Dose-dependent effect of cannabinoid WIN-55,212-2 on myelin repair following a demyelinating insult. *Sci Rep* **10**, 590.

[93] He X, Huang Y, Li B, Gong CX, Schuchman EH (2010) Deregulation of sphingolipid metabolism in Alzheimer's disease. *Neurobiol Aging* **31**, 398-408.

[94] Couttas TA, Kain N, Daniels B, Lim XY, Shepherd C, Kril J, Pickford R, Li H, Garner B, Don AS (2014) Loss of the neuroprotective factor Sphingosine 1-phosphate early in Alzheimer's disease pathogenesis. *Acta Neuropathol Commun* **2**, 9.

[95] Chen C (2023) Inhibiting degradation of 2-arachidonoylglycerol as a therapeutic strategy for neurodegenerative diseases. *Pharmacol Ther* **244**, 108394.

[96] Hurst DP, Schmeisser M, Reggio PH (2013) Endogenous lipid activated G protein-coupled receptors: emerging structural features from crystallography and molecular dynamics simulations. *Chem Phys Lipids* **169**, 46-56.

[97] Hait NC, Maiti A (2017) The Role of Sphingosine-1-Phosphate and Ceramide-1-Phosphate in Inflammation and Cancer. *Mediators Inflamm* **2017**, 4806541.

[98] Sanchez C, Rueda D, Segui B, Galve-Roperh I, Levade T, Guzman M (2001) The CB(1) cannabinoid receptor of astrocytes is coupled to sphingomyelin hydrolysis through the adaptor protein fan. *Mol Pharmacol* **59**, 955-959.

[99] Rahman SA, Gathungu RM, Marur VR, St Hilaire MA, Scheuermaier K, Belenky M, Struble JS, Czeisler CA, Lockley SW, Klerman EB, Duffy JF, Kristal BS (2023) Age-related changes in circadian regulation of the human plasma lipidome. *Commun Biol* **6**, 756.

[100] Yang S, Park JH, Lu HC (2023) Axonal energy metabolism, and the effects in aging and neurodegenerative diseases. *Mol Neurodegener* **18**, 49.

[101] Stahon KE, Bastian C, Griffith S, Kidd GJ, Brunet S, Baltan S (2016) Age-Related Changes in Axonal and Mitochondrial Ultrastructure and Function in White Matter. *J Neurosci* **36**, 9990-10001.

[102] Lee JY, Harney DJ, Teo JD, Kwok JB, Sutherland GT, Larance M, Don AS (2023) The major TMEM106B dementia risk allele affects TMEM106B protein levels, fibril formation, and myelin lipid homeostasis in the ageing human hippocampus. *Mol Neurodegener* **18**, 63.

[103] Shokhirev MN, Johnson AA (2022) An integrative machine-learning meta-analysis of high-throughput omics data identifies age-specific hallmarks of Alzheimer's disease. *Ageing Res Rev* **81**, 101721.

[104] Chew H, Solomon VA, Fonteh AN (2020) Involvement of Lipids in Alzheimer's Disease Pathology and Potential Therapies. *Front Physiol* **11**, 598.

[105] Blank M, Enzlein T, Hopf C (2022) LPS-induced lipid alterations in microglia revealed by MALDI mass spectrometry-based cell fingerprinting in neuroinflammation studies. *Sci Rep* **12**, 2908.

[106] Jarmusch AK, Alfaro CM, Pirro V, Hattab EM, Cohen-Gadol AA, Cooks RG (2016) Differential Lipid Profiles of Normal Human Brain Matter and Gliomas by Positive and Negative Mode Desorption Electrospray Ionization - Mass Spectrometry Imaging. *PLoS One* **11**, e0163180.

[107] Rothman SM, Tanis KQ, Gandhi P, Malkov V, Marcus J, Pearson M, Stevens R, Gilliland J, Ware C, Mahadomrongkul V, O'Loughlin E, Zeballos G, Smith R, Howell BJ, Klappenbach J, Kennedy M, Mirescu C (2018) Human Alzheimer's disease gene expression signatures and immune profile in APP mouse models: a discrete transcriptomic view of Abeta plaque pathology. *J Neuroinflammation* **15**, 256.

[108] Blank M, Hopf C (2021) Spatially resolved mass spectrometry analysis of amyloid plaque-associated lipids. *J Neurochem* **159**, 330-342.

[109] Ge J, Koutarapu S, Jha D, Dulewicz M, Zetterberg H, Blennow K, Hanrieder J (2023) Tetramodal Chemical Imaging Delineates the Lipid-Amyloid Peptide Interplay at Single Plaques in Transgenic Alzheimer's Disease Models. *Anal Chem* **95**, 4692-4702.

[110] Michno W, Wehrli PM, Koutarapu S, Marsching C, Minta K, Ge J, Meyer SW, Zetterberg H, Blennow K, Henkel C, Oetjen J, Hopf C, Hanrieder J (2022) Structural amyloid plaque polymorphism is associated with distinct lipid accumulations revealed by trapped ion mobility mass spectrometry imaging. *J Neurochem* **160**, 482-498.

[111] Mufson EJ, Binder L, Counts SE, DeKosky ST, de Toledo-Morrell L, Ginsberg SD, Ikonomovic MD, Perez SE, Scheff SW (2012) Mild cognitive impairment: pathology and mechanisms. *Acta Neuropathol* **123**, 13-30.

[112] Bennett DA, Wilson RS, Boyle PA, Buchman AS, Schneider JA (2012) Relation of neuropathology to cognition in persons without cognitive impairment. *Ann Neurol* **72**, 599-609.

[113] DeKosky ST, Ikonomovic MD, Styren SD, Beckett L, Wisniewski S, Bennett DA, Cochran EJ, Kordower JH, Mufson EJ (2002) Upregulation of choline acetyltransferase activity in hippocampus and frontal cortex of elderly subjects with mild cognitive impairment. *Ann Neurol* **51**, 145-155.

[114] Davis KL, Mohs RC, Marin D, Purohit DP, Perl DP, Lantz M, Austin G, Haroutunian V (1999) Cholinergic markers in elderly patients with early signs of Alzheimer disease. *JAMA* **281**, 1401-1406.

[115] Bennett DA, Schneider JA, Wilson RS, Bienias JL, Arnold SE (2004) Neurofibrillary tangles mediate the association of amyloid load with clinical Alzheimer disease and level of cognitive function. *Arch Neurol* **61**, 378-384.

Table 1. Demographic, Cognitive, and Neuropathological Variables Stratified by Clinical Group.

	YAC (n=6)	NCI (n = 5)	MCI (n = 5)	AD (n = 5)	P-value	Groupwise Comparisons
Age at Death (years) (range)	68.83±7.94 (58-79)	86.27±4.85 (79-90)	83.32±7.44 (72-92)	92.04±8.54 (80-101)	0.004	YAC<NCI
Education (years) (range)	n/a	18.60±2.97 (15, 22)	19.60±1.82 (18, 22)	17.80±3.11 (14, 21)	0.69	ns
Sex (M/F)	4/2	1/4	2/3	2/3	0.74	ns
APOE ε4 (Carrier/Non-Carrier)	n/a	1/4	0/5	2/3	0.29	ns
MMSE (range)	n/a	27.80±0.84 (27, 29)	28.2±2.17 (25, 30)	17.80±4.15 (15, 24)	0.008	NCI, MCI>AD
Global Cognitive Score (z-score) (range)	n/a	0.04±0.27 (-0.24, 0.43)	-0.29±0.43 (-0.95, 0.15)	-1.36±1.01 (-2.45, 0.08)	0.05	NCI>AD
Episodic Memory (z-score) (range)	n/a	0.39±0.39 (-0.17, 0.85)	-0.24±0.86 (-1.46, 0.93)	-1.67±1.35 (-3.0, 0.07)	0.04	NCI>AD
Semantic Memory (z-score) (range)	n/a	-0.39±0.87 (-1.30, 0.59)	-0.30±0.48 (-0.84, 0.20)	-1.14±0.82 (-2.21, 0.06)	0.22	ns
Working Memory (z-score) (range)	n/a	0.16±0.27 (-0.19, 0.47)	-0.74±0.39 (-1.17, -0.17)	-1.00±1.14 (-2.14, 0.56)	0.07	ns
Perceptual Speed (z-score) (range)	n/a	-0.09±0.61 (-0.85, 0.42)	-0.39±0.35 (-0.99, -0.13)	-2.33±0.79 (-3.38, -1.43)	0.008	NCI>AD
Visuospatial (z-score) (range)	n/a	-0.19±0.78 (-0.61, 1.02)	-0.32±0.27 (-0.61, -0.02)	-0.82±1.31 (-2.12, 0.75)	0.75	ns
Post-Mortem Interval (hours) (range)	10.29±5.52 (4.8, 21)	4.67±1.86 (3, 9.9)	5.73±2.99 (2.4, 6.9)	5.53±3.79 (2.6, 12)	0.19	ns
Brain Weight (grams) (range)	1,235±122* (1100, 1375)	1,186±93.05 (1040, 1380)	1,192±133.68 (1095, 1310)	1,158±126.57 (1020, 1340)	0.75	ns
Braak Stage						
I-II	0	1	3	0	0.15	ns
III-IV	0	4	1	3		
V-VI	0	0	1	2		
CERAD						
No AD	n/a	2	3	0	0.09	ns
Possible AD		0	0	0		
Probable AD		3	0	3		
Definite AD		0	2	2		
NIA Reagan						
Not AD	n/a	0	0	0	0.20	ns
Low Likelihood		2	3	0		
Intermediate Likelihood		3	1	3		
High Likelihood		0	1	2		

*n=5, n/a: not applicable, ns: non-significant

Table 2. [^{35}S]GTPγS binding induced by WIN55,212-2 (10 µM), CYM-5442 (10 µM) and Carbachol (100 µM) in frontal cortex lamina and white matter of NCI, MCI and AD expressed in nCi/g t.e.

Brain region	NCI	MCI	AD
	CB1 receptor activity (nCi/g t.e.)		
Grey matter	260 ± 135	399.7 ± 176	402.1 ± 199
Layer I-II	179 ± 95	279 ± 114	512 ± 317
Layer III-IV	493 ± 228	383.7 ± 196	373.1 ± 208
Layer V-VI	420 ± 84	539.1 ± 130	700.2 ± 117*****
White matter	44.73 ± 33.54	77.2 ± 113	50.9 ± 29
	S1P1 receptor activity (nCi/g t.e.)		
Grey matter	1267 ± 309	1384 ± 309	1069 ± 379
Layer I-II	908 ± 446	921.9 ± 208	983.9 ± 315
Layer III-IV	1097 ± 358	1369 ± 535	1156 ± 426
Layer V-VI	1509 ± 288	1560 ± 405	1330 ± 404
White matter	662.9 ± 271	365.6 ± 148	224.3 ± 92*****
	M2/M4 receptor activity (nCi/g t.e.)		
Grey matter	146 ± 51	356 ± 91	70 ± 49##
Layer I-II	158 ± 113	144 ± 190	36 ± 62
Layer III-IV	142 ± 77	348 ± 189	180 ± 100
Layer V-VI	149 ± 83	335 ± 210	57 ± 25#
White matter	85 ± 82	77 ± 113	51 ± 29

Data is presented as the mean ± SEM, *****p<0.05 AD *vs* NCI, ##p<0.01 AD *vs* MCI.

724 **Figure 1.**

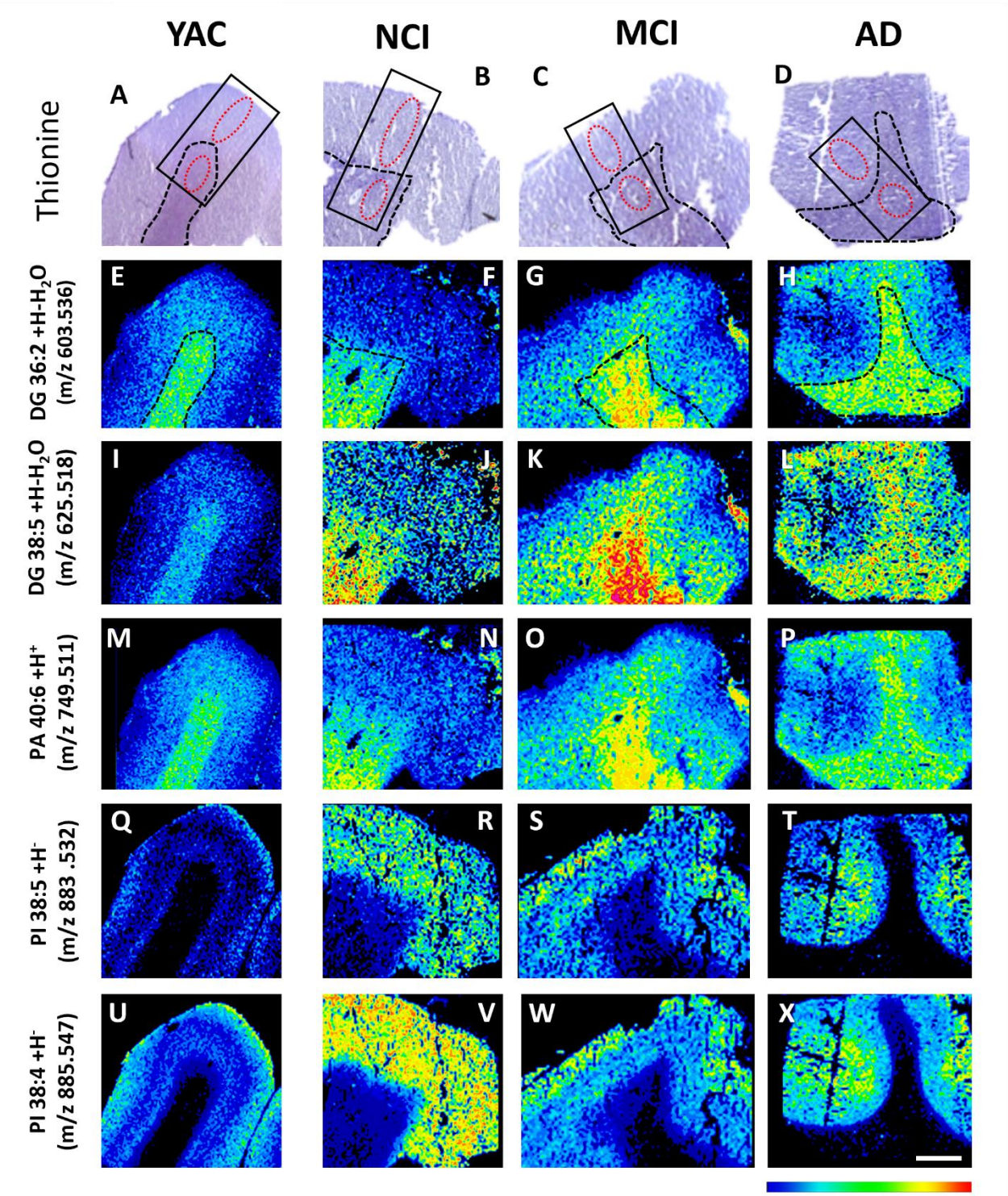

725

726

Figure 2.

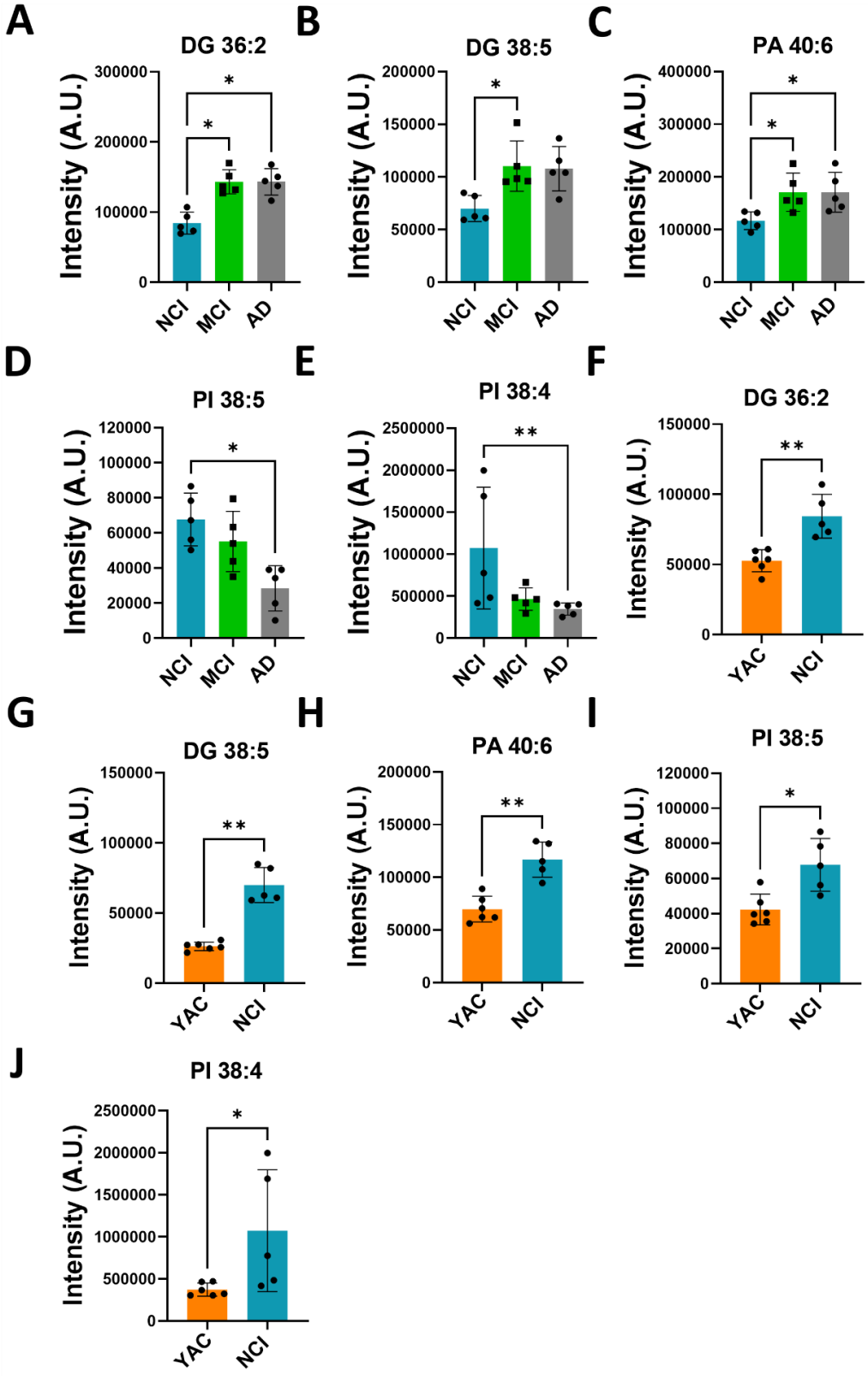
A
DG 36:2
Intensity (A.U.)
300000
200000
100000
0
NCI
MCI
AD
B
DG 38:5
200000
150000
100000
50000
C
PA 40:6
400000
300000
D
PI 38:5
120000
100000
80000
60000
40000
20000
E
PI 38:4
2500000
2000000
1500000
1000000
500000
F
DG 36:2
150000
50000
YAC
G
DG 38:5
H
PA 40:6
I
PI 38:5
J
PI 38:4

729 **Figure 3.**

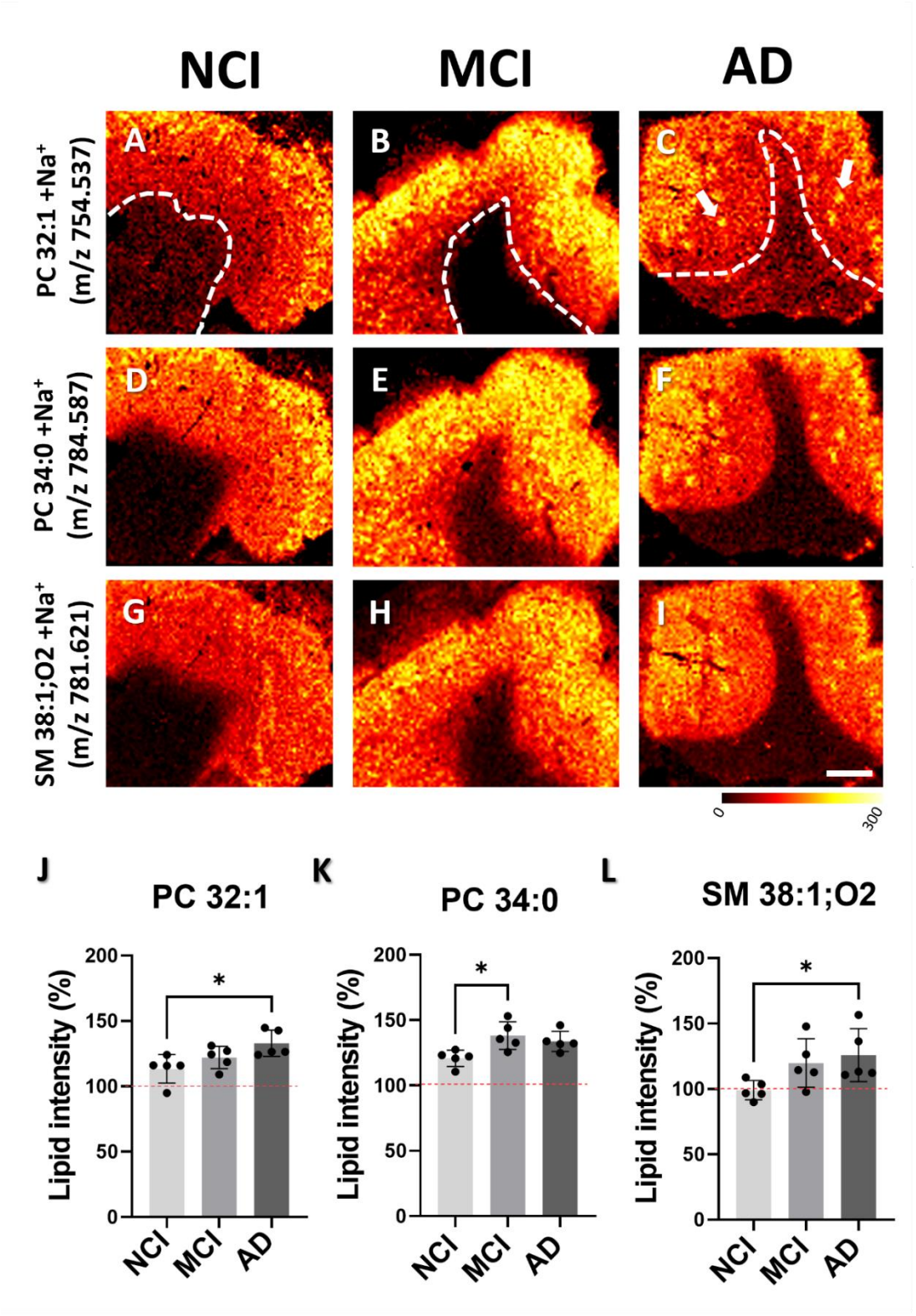

730

731

Figure 4.

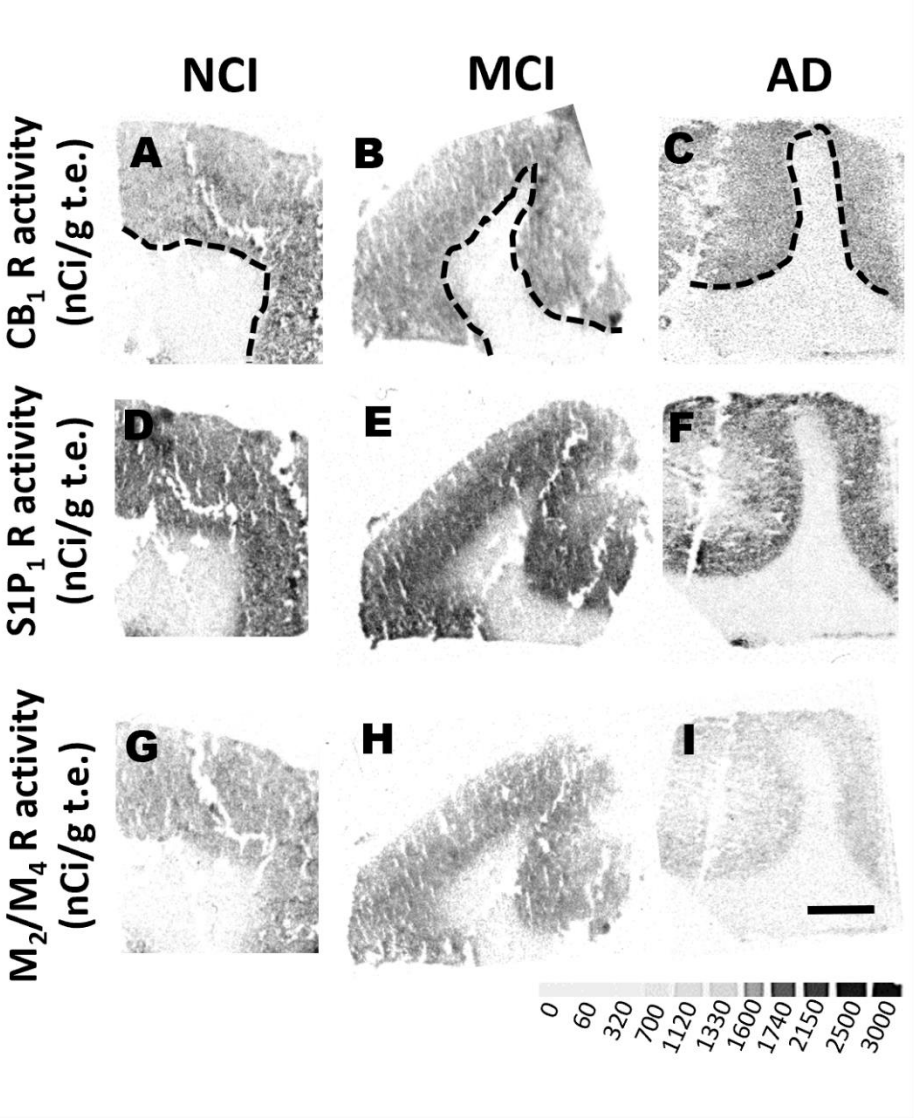
NCI
MCI
AD
CB1 R activity (nCi/g t.e.)
S1P1 R activity (nCi/g t.e.)
M2/M4 R activity (nCi/g t.e.)
A
B
C
D
E
F
G
H
I
0
60
320
700
1120
1330
1600
1740
2150
2500
3000

740 **Figure 5.**

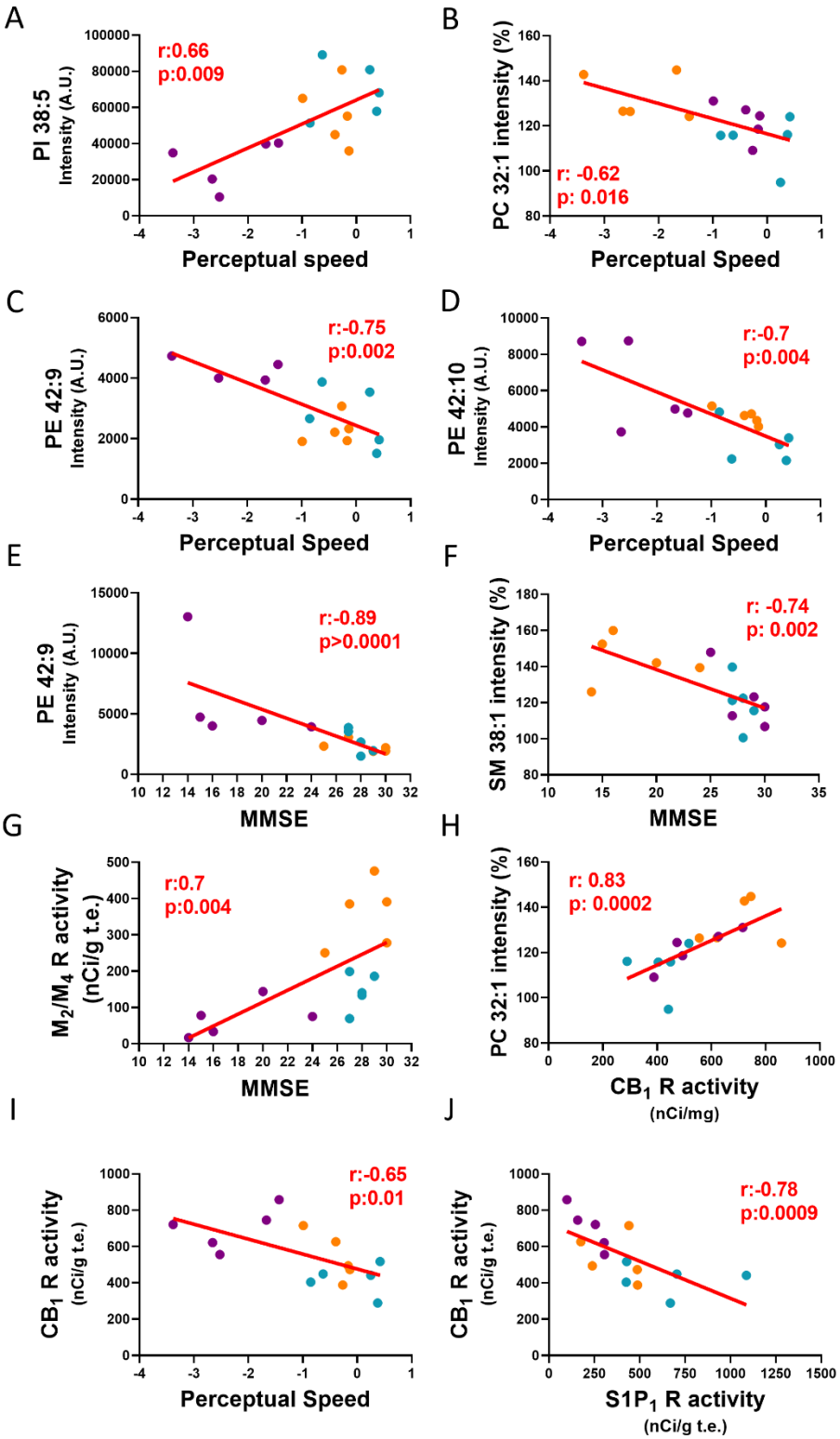

741

Figure legends

Fig. 1. Sections showing MALDI-MSI ion lipid species distribution counterstained with Thionine-showing significant differences in frontal cortex WM intensities between YAC, NCI, MCI and AD cases. In the thionine-stained sections the rectangle (black box) indicates the area scanned by MALDI-MSI and the red oval denotes the area exported for analysis from a YAC (A), NCI (B), MCI (C) and an AD (D) case. MALDI-MSI color images of the distribution of diacylglycerol (DG) 36:2 (E-H), 38:5 (I-L), phosphatidic acid (PA) 40:6 (M-P), phosphatidylinositol (PI) 38:5 (Q-T), 38:4 (U-X) in the FC. Note that all lipids displayed an increase in intensity in the older NCI (F, J, N, R and V) compared to YAC (E, I, M, Q and U) cases. WM intensity of DG 36:2, 38:5 and PA 40:6 was significantly higher in MCI (G, K and O) compared to NCI (F, J and N) cases while WM intensity of PI 38:5 and 38:4 was significantly lower in AD (T and X) compared to NCI (R and V). Scale bar = 4 mm. Multi-colored ion intensity scale values: DG 36:2 = 0 – 4 x 10^5 A.U, DG 38:5 = 0 – 2 x 10^5 A.U, PA 40:6 = 0 – 3 x 10^5 A.U, PI 38:5 = 0 – 2 x 10^5 A.U and PI 38:4 = 0 – 3 x 10^7 A.U.

Fig. 2. Histograms showing MALDI-MSI lipid intensity in frontal cortex WM for YAC, NCI, MCI and AD cases. (A-E) Significant differences of lipids, obtained by the average of absolute intensities in arbitrary units (A.U.) of WM between NCI, MCI and AD were shown in panels, while (F-J) significant differences between YAC and NCI were shown in panels. **p<0.01, *p<0.05. Abbreviations: DG = Diacylglycerol, PA = phosphatidic acid, PI = phosphatidylinositol.

Fig. 3. MALDI-MSI ion distribution images and histograms showing differences in the intensities of lipid patches in GM between NCI, MCI and AD cases. (A-C) GM images, above dashed line, show the distribution of PC 32:1, (D-F) SM 38:1 and (G-I) PC 34:0. (J-L) Histograms display percentage of changes in lipid intensity across NCI, MCI and AD cases. Percent change in lipid intensity was determined

764 by comparing areas within the GM with no accumulation (100 %) to those with lipid accumulations. Red
765 dashed line indicates background level. Scale bar in panel I = 4 mm. Multicolored scale bar below panel
766 I indicates changes in intensity level. Abbreviations: PC = phosphatidylcholine and SM = sphingomyelin.

767 **Fig. 4. Functional autoradiographic images of lipid related receptors.** Representative
768 autoradiographic images of frontal cortex activity for CB_1R (A-D), $S1P_1R$ (E-J) and M_2/M_4 activity
769 stimulated by WIN55,212-2, CYM-5442 and carbachol (K-L) showing differences in GTPγS binding in
770 GM and WM in NCI, MCI and AD cases. Dashed line differentiates GM from WM. Scale bar in I = 4
771 mm. Grayscale bar below panel I indicates levels of GTPγS binding (nCi/g t.e.).

772 **Fig. 5. Linear regression graphs show associations between lipids intensities, receptor activity and**
773 **cognitive performance tests.** (A) Associations between perceptual speed and PI 38:5 intensity A.U., (B)
774 PC 32:1 intensity (%), (C) PE 42:9 intensity A.U. (D) PE 42:10 intensity A.U. (E) MMSE and PE 42:9
775 intensity A.U., (F) SM 38:1 intensity (%), (G) M_2/M_4 receptor activity. (H) CB_1 receptor activity in GM
776 layers V-VI and PC 32:1 intensity (%), (I) perceptual speed and (J) $S1P_1$ receptor activity in WM. Blue
777 dots correspond to NCI, orange dots to MCI and purple dots to AD. Abbreviations: PI =
778 Phosphatidylinositol, PE = Phosphatidylethanolamine, PC = phosphatidylcholine and SM =
779 sphingomyelin.

780

781

782

Barrow Neurological Institute | Dignity Health. St. Joseph's Hospital and Medical Center

Feb. 19, 2024

Dr. George Perry
Editor in Chief
Journal of Alzheimer's Disease

Dear Dr. Perry:

We have addressed the second reviewer's comments related to our article entitled "Frontal cortex lipid alterations during the onset of Alzheimer's disease." Each response is enumerated below:

Reviewer: 2

Comment 1. In figure 3 and supplementary figure 1, the authors are still missing a clear definition of the region that defines 100%. The figure legends state that this 100% value is the background, but to the reader "background" sounds like a region outside of the tissue. Please provide a better description of what exactly is meant by background in the figure legends. I assume this refers to the "areas not containing similar accumulation", as described in the methods. So, is the percentage intensity for lipid islands in these figures expressed relative to regions of the grey matter that do not contain these lipid islands?

Author reply

We thank the reviewer for the comment. We clarified the use of the word "background" in figure legend 3 as follows:

"Percent change in lipid intensity was determined by comparing areas within the GM with no accumulation (100 %) to those with lipid accumulations."

Comment 2. The legend to figure 1 is still incorrect in the description of parts E to X. The authors have defined the lipids that are shown in each set of four images, but refer to a significant increase in these lipids: "MALDI-MSI color images show a significant increase in diacylglycerol (DG) 36:2 (E-H), 38:5 (I-L), phosphatidic acid (PA) 40:6 (M-P),

phosphatidylinositol (PI) 38:5 (Q-T), 38:4 (U-X) in the FC WM (black dashed lines)". Firstly, what significant increase are you referring to? A significant increase in WM of the AD cases relative to the NCI? Secondly, not all of these lipids showed the same trend between the sample groups. Figure 2 shows a decrease in the PI species. Perhaps the authors should opt for a more descriptive figure legend, e.g. "MALDI-MSI example images for diacylglycerol (DG) 36:2 (E-H), DG(38:5) (I-L), phosphatidic acid (PA) 40:6 (M-P), phosphatidylinositol (PI) 38:5 (Q-T), and PI(38:4) (U-X) in the FC of YAC (E,I,M, Q, U), NCI (F, J, N, R, V), ... cases.

Author reply

We thank the reviewer for the comment and have clarified Figure legend 1 to read:

"Note that all lipids displayed an increase in intensity in the older NCI (F, J, N, R and V) compared to YAC (E, I, M, Q and U) cases. WM intensity of DG 36:2, 38:5 and PA 40:6 was significantly higher in MCI (G, K and O) compared to NCI (F, J and N) cases while WM intensity of PI 38:5 and 38:4 was significantly lower in AD (T and X) compared to NCI (R and V).".

Sincerely,

Elliott

Elliott J. Mufson, Ph.D.
Director, Alzheimer's Disease Research Laboratory
Greening Chair in Neuroscience
Professor, Department of Neurobiology
Barrow Neurological Institute
350 W. Thomas Rd.
Phoenix, AZ 85013
Phone: 602-406-8525
Fax: 602-406-8520
email: elliott.mufson@barrowneuro.org

Frontal cortex lipid alterations during the onset of Alzheimer's disease

Marta **Moreno-Rodriguez**[a], Sylvia E. **Perez**[a], Jonatan **Martinez-Gardeazabal**[b], Ivan **Manuel**[b], Michael **Malek-Ahmadi**[c], Rafael **Rodriguez-Puertas**[b]*, Elliott J. **Mufson**[a,d]*

a. Department of Translational Neuroscience, Barrow Neurological Institute, Phoenix 85013, AZ, USA.
b. Department of Pharmacology, Fac. of Medicine and Nursing, University of the Basque Country. 48949 Leioa, Spain.
c. Banner Alzheimer's Institute, Phoenix, 85006, AZ, USA
d. Departments of Translational Neuroscience and Neurology, Barrow Neurological Institute, Phoenix 85013, AZ, USA.

*****Both authors contributed equally to the overall direction and planning of the research

Running Title: Frontal cortex lipid activity in Alzheimer's disease

Corresponding author:

Elliott J. Mufson, Ph.D.
Director, Alzheimer's Disease Research Laboratory
Greening Chair in Neuroscience
Professor, Department of Neurobiology
Barrow Neurological Institute
350 W. Thomas Rd.
Phoenix, AZ 85013
Phone: 602-406-8525
Fax: 602-406-8520
email: elliott.mufson@barrowneuro.org

Abstract

Background: Although sporadic Alzheimer's disease (AD) is a neurodegenerative disorder of unknown etiology, familial AD (FAD) is associated with specific gene mutations. A commonality between these forms of AD is that both display multiple pathogenic events including cholinergic and lipid dysregulation.

Objective: We aimed to identify the relevant lipids and the activity of their related receptors in the frontal cortex, correlating them with cognitive function throughout the progression of AD.

Methods: MALDI-Mass Spectrometry Imaging (MSI) and functional autoradiography was used to evaluate the distribution of phospholipids/sphingolipids and the activity of cannabinoid 1 (CB_1), sphingosine 1-phosphate 1 ($S1P_1$) and muscarinic M_2/M_4 receptors in the frontal cortex (FC) of people that come to autopsy with premortem clinical diagnosis of AD, mild cognitive impairment (MCI) and no cognitive impairment (NCI).

Results: MALDI-MSI revealed an increase in myelin-related lipids, such as diacylglycerol (DG) 36:1, DG 38:5 and phosphatidic acid (PA) 40:6 in the white matter (WM) in MCI compared to NCI, and a downregulation of WM phosphatidylinositol (PI) 38:4 and PI 38:5 levels in AD compared to NCI. Interestingly, elevated levels of phosphatidylcholine (PC) 32:1, PC 34:0, and sphingomyelin (SM) 38:1 were observed in discrete lipid accumulations in the FC supragranular layers during disease progression. Muscarinic M_2/M_4 receptor activation in layers V-VI decreased in AD compared to MCI. CB_1 receptor activity was upregulated in layers V-VI, while $S1P_1$ was downregulated within WM in AD relative to NCI.

Conclusions: FC WM lipidomic alterations are associated with myelin dyshomeostasis in prodromal AD, suggesting WM lipid maintenance as a potential therapeutic target for dementia.

Keywords: Alzheimer's disease, MALDI-MSI, lipidomic, cholinergic, mild cognitive impairment, muscarinic receptor, autoradiography

INTRODUCTION

Alzheimer's disease (AD) is the most common type of dementia, characterized by a progressive deterioration of cognitive function. In addition to the beta-amyloid (Aβ) plaques, neurofibrillary tangles and central cholinergic deficits, clinical and epidemiological investigations have linked disrupted lipid metabolism with the pathogenesis and progression of AD [1]. Previous studies using lipid extractions have shown decreases in cortical polyunsaturated fatty acids (PUFA) and monounsaturated fatty acids (MUFA) in AD [2]. Docosahexaenoic acid (DHA) and arachidonic acid (AA), which are the most abundant brain PUFAs are downregulated in hippocampus [3], cortical levels of phosphatidylcholine (PC), phosphatidylinositol (PI) and phosphatidylethanolamine (PE) are reduced, while diacylglycerols (DG) increase [4, 5] in AD. Sphingomyelin (SM), galactosylceramides, and sulfatides, important components of myelination, are lower in cortical areas in AD and subjects with very mild dementia [6-9]. In addition, a loss of ceramide synthase 2, that produces very long acyl chain lipids of myelin, precedes neurofibrillary tangle pathology in temporal and frontal cortical grey matter (GM) in AD [10]. Despite evidence of lipidomic dysregulation, its role in the pathogenesis of AD remains unexplored. During the past several years the development of matrix-assisted laser desorption/ionization mass spectrometry imaging (MALDI-MSI), which is capable of the simultaneous visualization of the spatial distribution of hundreds of thousands of lipids in a label-free manner [11-13] provided a new tool for the investigation of lipids in AD. For example, MALDI-MSI was employed to investigate the spatial correlation of lipids within Aβ plaques [14, 15] and to discover novel therapeutic approaches centered around the modulation of lipid signaling in AD animal models [16-18]. The application of MALDI-MSI based lipidomic research

reported a reduction of sulfatides, myelin specific lipids in the FC [19] and a decrease of DHA-containing PC in temporal gray matter of late-stage AD patients [20, 21].

The FC, a component of the default mode network (DMN) [22], which plays a key role in the modulation of episodic memory, displays cholinergic deficits and alterations in choline-containing lipids (e.g., PC and SM) in AD [23, 24]. However, the relationship between lipid and cholinergic dysregulation during the onset of AD remains unknown. Disruption in lipid homeostasis may lead to cholinergic dysfunction, due changes in phospholipid and sphingolipid pathways that are critical for cell membrane repair and production of the neurotransmitter acetylcholine (ACh), which are affected in AD [25, 26]. Since cannabinoid 1 (CB_1) and sphingosine 1-phosphate 1 ($S1P_1$) receptors are the most widespread lipidic neuromodulators within the central nervous system and their endogenous ligands are derived from membrane lipid precursors, changes in the activity of these receptors likely play a key role in the modification of lipid homeostasis [27-29], which may be altered in AD. In this regard, CB_1 activity is increased following basal forebrain cholinergic denervation [30] and the modulation of the release of ACh in rat cortex [31], suggesting an interaction between cannabinoid and cholinergic systems resulting from cannabinoid activation via muscarinic receptors [32, 33]. Although FC CB_1 receptor activity is alter in AD [34] and even upregulated in the early stages of the disease [35, 36], others report no change or a decrease in sporadic AD [37, 38]. However, lysophospholipid $S1P_1$, which is also activated after cholinergic muscarinic signaling [33] is decreased in the superficial layers of the FC in severe AD [39]. Therefore, the aim of the present study was to identify early lipid dysregulation within grey and white matter (WM) and their relationship with CB_1, $S1P_1$ and muscarinic receptor activity in the FC during the onset of AD, using MALDI-MSI and functional autoradiography.

MATERIALS AND METHODS

Subjects

The study included 15 cases with a *premortem* clinical diagnosis of no cognitive impairment (NCI, n = 5; 86.27 ± 4.8 years), mild cognitive impairment (MCI, n = 5; 83.32 ± 7.4 years) and mild to moderate AD (AD, n = 5; 92.04 ± 5.4 years) from the Rush Religious Orders Study (RROS) and 6 younger-aged controls (YAC, 68.83 ± 7.9 years) non cognitively impaired Braak stage 0 cases from the Biobank of the Basque Country and Asturias Central University Hospital (see Table 1).

The Human Research Committees of Rush University Medical Center and Dignity Health approved this study and written informed consent for research and brain autopsy was obtained from the participants or their family/guardians. The YAC samples were obtained at autopsy following informed consent in accordance with the ethics committees of the University of the Basque Country (UPV/EHU) (CEISH/244MR/2015/RODRIGUEZ PUERTAS), following the Code of Ethics of the World Medical Association (Declaration of Helsinki) and warranting the privacy rights of the human subjects.

Clinical and Neuropathological Evaluation

The demographic, clinical and neuropathological characteristics of the cases provided by the RROS and the Biobank of the Basque Country and Asturias Central University Hospital are presented in Table 1. Although a similar detailed clinical evaluation was not available for the YAC cases, there was no evidence of cognitive difficulties or neurological disease in their medical records. Clinical criteria for NCI, MCI, and AD RROS cases have been reported in numerous previous publications [40, 41]. Here we provide an overview of the RROS clinical evaluation process. The RROS clinical evaluation was designed to determine the presence of dementia and its etiology, with particular attention paid to Alzheimer's disease (AD). Examination of medical history included uniform, structured questions about cognitive decline, stroke, Parkinson's disease, head injury, tumor, depression, and other medical problems. Medications used

within the previous 14 days of examination were reviewed. A uniform structured neurologic examination was carried out by trained nurse clinicians and neuropsychology technicians administered a battery of cognitive tests. Tests were chosen to assess a range of cognitive tasks with an emphasis on those affected by aging and AD (e.g., Mini-Mental State Examination (MMSE) [42], the CERAD neuropsychological measures: Verbal Fluency, Boston Naming, Word List Memory, Word List Recall and Word List Recognition [43], oral version of Symbol Digit Modalities Test [44], Logical Memory (Story A) and Digit Span subtests of the Wechsler Memory Scale-Revised [45], Complex Ideational Material [46], Judgment of Line Orientation [47], and subsets of items from the Standard Progressive Matrices [48]. A caveat of neuropsychological tests is that they do not measure cognition uniformly across different levels of education, educationally adjusted cut points were used for rating impairment on each test based on prior test use and existing reports in the literature. A computer algorithm applies these cut points uniformly and converted each participant's score into deficit ratings in five cognitive domains (orientation, attention, memory, language and perception) [49, 50]. An impaired score was developed for each domain that entailed dysfunction on several tests within that domain. A board-certified neuropsychologist, blinded to a participant's demographics, clinical data except education, occupation, and information about sensory or motor deficits used these findings to summarize deficits in each of the five cognitive domains as probable, possible or not present. For those cases with borderline dementia an opinion regarding the probability of dementia and AD is made by the neuropsychologist. A clinical diagnosis was then made by a board-certified neurologist with expertise in the evaluation of older people in combination with a neuropsychologist's opinion of cognitive impairment and the presence of dementia. The diagnosis of dementia and AD was made based upon the recommendations of the joint working group of the National Institute of Neurological and Communicative Disorders and the Stroke and the Alzheimer's Disease and Related Disorders Association (NINCDS/ADRDA) [51]. MCI criteria are compatible with those used by

many others to describe persons who are not cognitively normal but fail to meet accepted criteria for dementia [52-54]. Here, MCI was defined as those persons rated as impaired on neuropsychological testing by the neuropsychologist but were not determined to be demented by the examining neurologist. Average time from the last clinical evaluation to death was ~ 8 months.

Postmortem neuropathology for the RROS cases was performed as reported previously [41, 55], which included Braak staging [56], NIA-Reagan criteria [57], and the Consortium to Establish a Registry for Alzheimer's Disease (CERAD) [58]. A board-certified neuropathologist excluded cases with other pathologies (e.g., cerebral amyloid angiopathy, vascular dementia, dementia with Lewy bodies, hippocampal sclerosis, Parkinson's disease, and large strokes) and those treated with acetylcholinesterase inhibitors.

Cortical samples

Frontal cortex samples from Brodmann area 9, which contained the superior longitudinal WM tract, were immediately frozen at -80°C, cut into 20 µm thick sections onto gelatin-coated slides using a cryostat (Microm HM550, Walldorf, Germany) and stored at -25 °C prior autoradiography and MALDI-MSI assay. Functional autoradiography of M_2/M_4, CB_1 and $S1P_1$ receptors were performed using tissue from NCI, MCI, and AD. However, MALDI-MSI was performed in tissue obtained from the YAC, NCI, MCI, and AD groups.

MALDI-MSI

We used matrix-assisted laser desorption ionization as an imaging mass spectrometry method (MALDI – MSI) for the analysis of the lipid composition and anatomical distribution within FC GM and WM. Prior to the lipid analysis, sections from all cases, were sprayed (six passes) with cyano-4-hydroxycinnamic

acid (CHCA) as a chemical matrix at 10 mg/ml concentration in 50 % methanol using a Tissue MALDI sprayer (TM sprayer, HTX Technologies, LCC, Carrboro, NC, USA) with a flow rate of 120 ml/min and at 70ºC. We scanned the samples in both positive and negative ionization mode, in the range of m/z 500 – 1300 with a LTQ – Orbitrap – XL mass spectrometer (Thermo Fisher Scientific, San Jose), equipped with a nitrogen laser of λ = 337 nm, using a repetition rate = 60 Hz and a spot size= 80 × 120 µm. The scanned parameters were 2 µscans/step with 10 laser shots and a raster step size of 100 µm at laser fluency of 15 - 40 µJ.

The area scanned in each group included all cortical layers and WM (Fig. 1 A-D, region outlined by black box). For statistical analysis, lipid intensities in the white and gray matter delimited by red circles (Fig. 1 A-D) were exported separately in positive and negative ions using MSiReader software [59], as the average of absolute intensity in arbitrary units from each area and ionization mode. In addition, we exported the intensities from 5 lipid islands and 5 areas not containing similar accumulation within the GM in the positive ion mode. Lipid assignment was performed based on the m/z values with a 5-ppm mass accuracy as the tolerance window [60] using Lipid Maps (www.lipidmaps.org) or the Human metabolome Database (www.hmdb.ca) [59, 61] and reported previously [62-66]. For illustrative purposes, a section from each group was first scanned and then counterstained with thionine to aid in cytoarchitectonic determination [60] (see Fig. 1).

Functional autoradiography of activated $G\alpha_{i/o}$ proteins using a [^{35}S] GTPγS binding assay

Frozen sections from each case were dried, followed by two consecutive incubations in HEPES-based buffer (50 mM HEPES, 100 mM NaCl, 3 mM $MgCl_2$, 0.2 mM EGTA and 1% BSA, pH 7.4) for 30 min at 30°C to remove endogenous ligands. Briefly, sections were incubated for 2 h at 30°C in the same buffer

supplemented with 2 mM GDP, 1 mM DTT (Sigma, St. Louis, MO, USA) and 0.04 nM [^{35}S] GTPγS (initial specific activity 1250 Ci/mmol, Perkin Elmer, Boston, MA, USA). Basal binding was determined in two consecutive sections in the absence of the agonist. Agonist-stimulated binding using the same reaction buffer was determined in a consecutive cut section in the presence of the corresponding receptor agonists, WIN55,212-2 (10 μM) for CB_1 receptors, carbachol (100 μM) for M_2/M_4 receptors and CYM-5442 (10 μM) for $S1P_1$ receptors (Sigma-Aldrich, St. Louis, MO, USA). Non-specific binding was defined by competition with GTPγS (10 μM) in a consecutively cut section. Sections were then washed twice in cold (4°C) 50 mM HEPES buffer (pH 7.4), dried and exposed to β-radiation sensitive film (Kodak Biomax MR, Sigma. St. Louis, MO, USA) together with a set of [^{14}C] standards calibrated for ^{35}S [17].

Statistical analysis

The Kruskal-Wallis test was used to assess between-group comparisons on demographic, cognitive, lipidomic variables and autoradiographic data for NCI, MCI, and AD cases. The Dunn's test was used to identify statistically significant groupwise comparisons. Since a formal adjustment for multiple comparisons was not applied to the lipidomic variables, we used a nominal significance level of alpha = 0.01 to balance a Type I error rate with the need to identify associations with possible biological relevance. The total number of lipids analyzed in each area of the FC in both positive and negative ionization mode were white matter positive, n = 393; white matter negative, n = 69; gray matter positive, n = 588; gray matter negative, n = 169. The five lipids that exhibited changes in FC WM in NCI, MCI, and AD cases, were compared between the YAC and NCI groups using a Mann-Whitney test with a significance level set at p = 0.05. Analysis comparing areas with lipid accumulation *versus* those without accumulation in all RROS cases was performed using a Mann-Whitney test with a nominal significance level of alpha =

0.01. This analysis revealed a reduced number of significantly different lipids (see supplementary Fig. 1). We conducted groupwise comparisons across clinical groups using a Kruskal-Wallis test followed by Dun's test, with the p-value set at 0.05. Spearman correlation assessed data associations and significance was set to 0.01 to account for multiple comparisons, while still allowing for an adequate number of associations to be deemed significant. Statistical analysis was conducted using R 4.2.3. Data was graphically represented using GraphPad Prism 9 (GraphPad Software, San Diego, CA, USA).

RESULTS

Subject Characteristics

The demographic, clinical, and neuropathological characteristics of the 15 Rush Religious Orders Study (RROS) participants used in this study were summarized in Table 1. There were no significant differences in age, sex, years of education, *postmortem* interval (PMI), brain weight, semantic memory, working memory, visuospatial speed z-score, or possession of at least one apolipoprotein (ApoE) ε4 allele across groups the RROS cases. Mini-Mental State Examination (MMSE) scores were significantly lower in the AD compared to the NCI and MCI groups. Global cognition, episodic memory and perceptual speed score were lower in AD compared to NCI. The YAC subjects were significantly younger than the RROS NCI cases (68.83 ± 7.9 *vs* 86.27 ± 4.8 years, respectively; Mann-Whitney test; $p = 0.004$). Although a similar clinical evaluation was not available for the YAC cases, a review of their medical records did not reveal evidence of cognitive difficulties or neurological disease. Moreover, all cases in the YAC subjects had a *postmortem* neuropathological Braak score of 0, while the NCI cases displayed an average Braak score of 3.2 ± 0.8 (see Table 1). A Braak score of 0 has been used to select control cases for analysis in clinical pathological studies [67].

Frontal cortex MALDI-MSI analysis in NCI, MCI and AD

We conducted MALDI-MSI analysis on frozen FC tissue obtained from elderly participants of the RROS that died with a clinical diagnosis of NCI, MCI, and AD and YAC cases with no cognitive impairment from the University of the Basque Country to identify phospholipids and sphingolipids by measuring the charged lipids in both positive and negative ions. Significant lipid changes were found only in the WM between clinical groups. The relative intensity levels of diacylglycerol (DG) 36:2 (Fig. 1 E-H, Fig. 2 A, $p<0.05$), DG 38:5 (Fig. 1 I-L, Fig. 2 B, $p<0.05$), and phosphatidic acid (PA) 40:6 (Fig. 1 M-P, Fig. 2 C, $p<0.05$) were significantly higher in MCI compared to elderly NCI cases, while phosphatidylinositol (PI) 38:5 (Fig. 1 Q-T, Fig. 2 D, $p<0.05$) and PI 38:4 (Fig. 1 U-X, Fig. 2 E, $p<0.01$) were lower in AD compared to NCI subjects. DG 36:2, DG 38:5, and PA 40:6 intensities were greater in WM compared to GM (Fig. 1 E-P), while PI 38:5 and PI 38:4, were more intense in GM than WM (Fig. 1 Q-X) in all experimental groups.

In addition, we also assessed the effect of differences in age between the NCI and YAC cases had upon FC lipid intensity. Here we found lower intensity levels of DG 36:2 (Fig. 1 E-F, Fig. 2 F, $p<0.01$), DG 38:5 (Fig. 1 I-J, Fig. 2 G, $p<0.01$), PA 40:6 (Fig. 1 M-N, Fig. 2 H, $p<0.01$), PI 38:5 (Fig. 1 Q-R, Fig. 2 I, $p<0.05$), and PI 38:4 (Fig. 1 U-V, Fig. 2 J, $p<0.05$) in YAC compared to NCI subjects.

Frontal cortex lipid accumulations in GM in NCI, MCI and AD

There was no difference in lipid composition in the GM across the groups. However, MALDI image analysis revealed discrete lipid patches in the supragranular layers of the GM (Supplementary Fig. S1), which displayed increased lipid intensity (%) for several phosphatidylcholines (PC) (PC 30:0, PC 32:0, PC 34:0, PC 32:1, PC 36:4, and PC 38:4) diacylglycerols (DG) (DG 30:0, DG 32:0, PC 34:0, DG

32:1, DG 34:3, DG 36:3, and DG 38:4), phosphatidic acids (PA) (PA 36:5, PA 36:4, PA 40:5, and PA 34:4) sphingomyelins (SM) (SM 36:1 and SM 38:1), ceramides (CER) (CER 36:1) and phosphatidylethanolamines (PE) (PE 40:7 and PE 44:12) and a downregulation of PA 36:2 and SM 42:2 compared to areas lacking these patches across all clinical groups (Supplementary Fig. S1). Conversely, only three lipids were increased between clinical groups. Specifically, PC 32:1 (Fig. 3 A-C, J, $p<0.05$) and SM 38:1 (Fig. 3 G-I, L, $p<0.05$) showed greater intensity in AD compared to NCI, while PC 34:0 (Fig. 3 D-F K, $p<0.05$) exhibited a significant elevation in MCI compared to NCI.

Frontal cortex functional autoradiography of activated $G\alpha_{i/o}$ proteins by the [^{35}S]GTPγS binding assay in NCI, MCI and AD cases

Functional coupling induced by carbachol for M_2/M_4-mediated receptor activity, was decreased in the FC GM in AD, specifically in layer V-VI compared to MCI. Additionally, [^{35}S]GTPγS binding induced by WIN55,212-2, primarily mediated by CB_1 activity, was increased in FC layer V-VI in AD compared to NCI. Lastly, functional coupling of $S1P_1$ receptors to $G_{i/o}$ proteins, induced by the specific agonist CYM5442, was reduced in FC WM in AD compared to NCI (Fig. 4 and Table 2).

Associations between lipids, receptor activity and demographic variables

A significant positive correlation was observed between PI 38:5 and perceptual speed (Fig. 5 A, $r = 0.66$, $p = 0.009$), while phosphatidylethanolamine (PE) 42:9 (Fig. 5 C, $r = -0.75$, $p = 0.002$) and PE 42:10 (Fig. 5 C, $r = -0.7$, $p = 0.004$) GM intensity levels negatively correlated with perceptual speed z-score values across clinical groups. PE 42:9 in GM correlated negatively with MMSE scores (Fig. 4 E, $r = -0.89$, $p<0.0001$). In addition, we found a positive correlation between the lipid intensity of the discrete oval accumulations of PC 32:1 and CB_1 stimulation in GM layers V-VI (Fig. 5 H, $r = 0.83$, $p=0.0002$). A negative correlation was found between PC 32:1 and perceptual speed across clinical groups (Fig. 5 B,

$r = -0.62$, $p = 0.016$). A negative correlation was found between sphingomyelin (SM) 38:1 (Fig. 5 F, $r = -0.74$, $p=0.002$) and MMSE across groups.

DISCUSSION

While multiple studies have demonstrated lipid alterations in the AD brain, the involvement of neurolipids together with their lipid precursors remain under-investigated during the progression of AD [68]. Here we showed significant lipid alterations in the WM in MCI, suggesting an early role in the onset of AD. Specifically, we found an increase in phosphatidic acid (PA) 40:6 and diacylglycerol (DG) 36:2 and DG 38:5 in MCI compared to NCI, and a decrease of phosphatidylinositol (PI) 38:5 and PI 38:4 in AD compared to NCI. The intensity of DGs and PA were higher in the WM compared to GM. Regarding the metabolic origins of DG and PA, phospholipid degradation emerges as a significant lipidomic pathway. PA and DG are important membrane lipids and second messengers that contribute to cellular processes either by their biophysical effect directly on the cell membrane or by recruiting proteins to the membrane [69]. The main pathway that regulates the formation and levels of these lipids is the phosphorylation of PI and activation of phospholipase C (PLC) to generate DG, which remains associated with the plasma membrane and generates PA [70]. Although numerous studies have documented the elevation of DGs in MCI [9, 71, 72], we found an increase within the WM in this prodromal stage suggesting that DGs are early indicators of WM damage. However, the precise mechanism(s) underlying the heightened levels of DG in the FC WM in MCI require further investigation. Additionally, we demonstrated decreased activity of M_2/M_4 receptors, stimulated by Carbachol, in layers V-VI in AD compared to MCI. Previous studies have shown a reduction in the density of total muscarinic receptors in cortical areas in AD [73]. In particular, pre-synaptic M_2 receptor density and G-protein coupling of this receptor was decreased in AD cortex [74, 75], supporting the current reduction of cortical muscarinic receptor activity in AD. In contrast, we found a non-significant trend for an increase in M_2/M_4 activity in

MCI compared to NCI. Interestingly, muscarinic receptors are known to mediate lipid signaling via the neurotransmitter ACh, which activates phospholipases to generate DG in synaptosomes both in *in vivo* and *in vitro* [76-78]. However, lipid signaling can be initiated through diverse pathways and receptors including cholinergic and non-cholinergic receptors [27-29] that modify phospholipases resulting in a localized accumulation of PA and DG. Accumulations of these lipid have been reported to modify the recruitment of proteins and fission processes related to WM membrane stability, which is detrimental to the maintenance of axonal connectivity [79, 80], results in a negative curvature to membrane bilayers due to their conical shape [81]. Perhaps increased levels of DG and PA are early indicators of WM dysfunction that, in part, underlie the cognitive deficits seen in prodromal AD.

Whether lipid modifications are associated with the onset of deficits in cognitive performance in AD is an under investigated area. In this regard, we found a downregulation of WM PI 38:5/38:4, which corresponds to arachidonic acid-enriched phosphatidylinositol (PI-AAs) (PI 18:0_20:4 and PI 18:1_20:4) [62, 63] in AD compared to NCI that correlated with impaired perceptual speed performance across groups. Evaluation of PI (18:0_20:4) images revealed more intense labeling in GM than WM. It has been reported that PIP_2 (18:0_20:4), resulting from the degradation of the PI-AA (18:0_20:4), was greater in WM myelin-enriched fractions [82] supporting the suggestion that alterations in phosphoinositide's and their respective regulatory pathways, play a role in WM and axon signaling dysfunction [83]. Another crucial regulatory pathway for PI (18:0_20:4) involves phospholipase A_2 (PLA_2), which maintains a balance between the conversion of arachidonic acid (AA) into proinflammatory mediators and reincorporation into PI-AA [84, 85]. AA, a key mediator of neuroinflammation, is elevated in AD and predominantly accumulates in the outer membrane of neurons and the myelin sheath [86] suggesting that the integrity of myelinated axons is compromised early in AD. Damage to the WM, which is comprised of 80% lipids, may disrupt neural transmission resulting in sensory, motor, and cognitive impairments

[86]. These findings are consistent with studies demonstrating disruption of WM in prodromal AD [87, 88]. We observed that the WM displayed a reduction of $S1P_1$ receptor activity, while CB_1 receptor activity within the infragranular layers of the grey matter which also contains heavily myelinated fibers [89, 90] are increased in AD compared to NCI. An imbalance between CB_1 and $S1P_1$ has been suggested to play a role in the maintenance of myelin integrity in AD [91, 92]. In this regard, alterations in the activity of these receptors may be attributed to changes in their endogenous agonists. For example, levels of the $S1P_1$ receptor agonist sphingosine 1 phosphate (S1P) are decreased in cortical grey and WM in early and advanced AD [93, 94], while signaling for the 2-arachidonoylglycerol (2-AG) an endocannabinoid endogenous CB_1 receptor agonist increases in response to Aβ plaques [95]. Both, CB_1 And $S1P_1$ receptor activity, negatively correlated while the temporal relationship or signaling crosstalk between these receptors remain unknown [96]. However, activation of CB_1 receptors drives the breakdown of sphingomyelin into ceramide, followed by its conversion to sphingosine. Subsequently, sphingosine is phosphorylated by sphingosine kinases to generate S1P, which binds to $S1P_1$ receptors [97, 98] suggesting that CB_1 receptors activate $S1P_1$ pathways in response to WM dysfunction.

Here, we also demonstrated that PA 40:6, DG 36:2, DG 38:5 and PI-AAs, which play a key role in WM myelination and maintenance, were significatively increased in older NCI compared to younger YAC subjects. Since myelinated axons in WM deteriorate structurally and functionally with age and are associated with poorer cognitive ability [99-102], an increase in PA 40:6, DG 36:2, DG 38:5 and PI-AA in NCI, suggests that normal physiological aging affects axonal and myelin lipids metabolism in the FC [103]. Although, we do not rule out the possibility that differences in ethnicity and lifestyle (i.e., diet and exercise) between YAC and NCI may influence the observed lipid changes with age in the WM [104], further investigation is needed to evaluate these lipid changes.

In the supragranular layers of the FC, patches of lipid displayed a significant increase in the intensity of PC 32:1, PC 34:0 and SM 38:1. Interestingly, PC 34:0 containing aggregates were seen in MCI, while both SM 38:1 and PC 32:1 were increased in AD. However, only the latter two lipids correlated with cognitive decline in AD. Each of these lipids are found in activated microglia [105], gliomas [106] and Aβ plaques in human and animal models of AD [14, 107-110]. Perhaps the upregulation of PC 32:1, PC 34:0 and SM 38:1 plays a key role in the pathogenesis of AD.

It is important to discuss limitations associated with the current study. For example, the small number of cases warrant a conservative interpretation of the findings requiring validation in a larger cohort, which would allow for correlations with ApoE genotypes, a major risk factor for the onset of AD and its neuropathologic lesions. It should be noted that the RROS participants were from a community-based population of highly educated retired clergy who had excellent health care and nutrition and were used in multiple clinical pathological [111, 112] and epidemiological investigations [41] of AD. However, other findings reported using tissue from the RROS cohort have not been found to be different from those derived from non-clerical populations [113, 114]. Individuals who volunteer may introduce bias by decreasing pathology, but this is partially overcome by the RROS high follow-up and autopsy rates [115]. Another caveat is that the YAC cases lacked a detailed pre-clinical evaluation. However, there was no evidence of impairment in cognition or adverse neurological disease documented in their medical records. On the other hand, all YAC cases were neuropathologically classified as Braak stage 0, indicative of no cognitive impairment [56]. "The possibility exists that differences in ethnicity and lifestyle (i.e., diet and exercise) may have influenced the observed difference in lipid values found between the YAC and NCI cases in the WM [103]. The influence that these cultural variables have upon lipid expression requires further investigation."

Strengths of this study include uniform *premortem* clinical and *postmortem* pathological evaluation and that final the pathologic classification was performed without knowledge of the clinical evaluation for the RROS cases.

In summary, the present findings provide evidence that lipidomic dysfunction is associated with the cognitive impairment seen in the prodromal phase of AD. The current findings indicate that modifications in WM myelin-related lipids and cholinergic receptors play a pivotal role in the onset of AD dementia and potentially serve as novel drug targets.

ACKNOWLEDGMENTS

We are indebted to the nuns, priests, and lay brothers who participated in the Rush Religious Orders Study and to the members of the Rush ADC. Technical and human support provided by University of the Basque Country (UPV/EHU), Ministry of Economy and Competitiveness (MINECO), Basque Government (GV/EJ), European Regional Development Fund (ERDF), and European Social Fund (ESF) and the collaboration of Ivan Fernandez is gratefully acknowledged. J.M.-G. is the recipient of "Margarita Salas" fellowship.

FUNDING

This study was supported by grants PO1AG014449, RO1AG043375, P30AG010161 and P30AG042146, RF1AG081286 from the National Institute on Aging, Barrow Neurological Institute and Arizona Alzheimer's Consortium. This work also was supported by grants from the regional Basque Government IT1454-22 to the "Neurochemistry and Neurodegeneration" consolidated research group and by Instituto

de Salud Carlos III through the project "PI20/00153" (co-funded by European Regional Development Fund "A way to make Europe") and by BIOEF project BIO22/ALZ/010 funded by Eitb Maratoia.

CONFLICT OF INTEREST

The authors declare no competing interests.

DATA AVALILABILITY

The data supporting the findings of this study are available within the article and in the supplementary material.

REFERENCES

[1] Yin F (2023) Lipid metabolism and Alzheimer's disease: clinical evidence, mechanistic link and therapeutic promise. *FEBS J* **290**, 1420-1453.

[2] Fabelo N, Martin V, Marin R, Moreno D, Ferrer I, Diaz M (2014) Altered lipid composition in cortical lipid rafts occurs at early stages of sporadic Alzheimer's disease and facilitates APP/BACE1 interactions. *Neurobiol Aging* **35**, 1801-1812.

[3] Prasad MR, Lovell MA, Yatin M, Dhillon H, Markesbery WR (1998) Regional membrane phospholipid alterations in Alzheimer's disease. *Neurochem Res* **23**, 81-88.

[4] Nitsch RM, Blusztajn JK, Pittas AG, Slack BE, Growdon JH, Wurtman RJ (1992) Evidence for a membrane defect in Alzheimer disease brain. *Proc Natl Acad Sci U S A* **89**, 1671-1675.

[5] Stokes CE, Hawthorne JN (1987) Reduced phosphoinositide concentrations in anterior temporal cortex of Alzheimer-diseased brains. *J Neurochem* **48**, 1018-1021.

[6] Han X, D MH, McKeel DW, Jr., Kelley J, Morris JC (2002) Substantial sulfatide deficiency and ceramide elevation in very early Alzheimer's disease: potential role in disease pathogenesis. *J Neurochem* **82**, 809-818.

[7] Soderberg M, Edlund C, Alafuzoff I, Kristensson K, Dallner G (1992) Lipid composition in different regions of the brain in Alzheimer's disease/senile dementia of Alzheimer's type. *J Neurochem* **59**, 1646-1653.

[8] Cheng H, Wang M, Li JL, Cairns NJ, Han X (2013) Specific changes of sulfatide levels in individuals with pre-clinical Alzheimer's disease: an early event in disease pathogenesis. *J Neurochem* **127**, 733-738.

[9] Wood PL, Medicherla S, Sheikh N, Terry B, Phillipps A, Kaye JA, Quinn JF, Woltjer RL (2015) Targeted Lipidomics of Fontal Cortex and Plasma Diacylglycerols (DAG) in Mild Cognitive Impairment and Alzheimer's Disease: Validation of DAG Accumulation Early in the Pathophysiology of Alzheimer's Disease. *J Alzheimers Dis* **48**, 537-546.

[10] Couttas TA, Kain N, Suchowerska AK, Quek LE, Turner N, Fath T, Garner B, Don AS (2016) Loss of ceramide synthase 2 activity, necessary for myelin biosynthesis, precedes tau pathology in the cortical pathogenesis of Alzheimer's disease. *Neurobiol Aging* **43**, 89-100.

[11] Hu H, Laskin J (2022) Emerging Computational Methods in Mass Spectrometry Imaging. *Adv Sci (Weinh)* **9**, e2203339.

[12] Schubert KO, Weiland F, Baune BT, Hoffmann P (2016) The use of MALDI-MSI in the investigation of psychiatric and neurodegenerative disorders: A review. *Proteomics* **16**, 1747-1758.

[13] Martinez-Gardeazabal J, Gonzalez de San Roman E, Moreno-Rodriguez M, Llorente-Ovejero A, Manuel I, Rodriguez-Puertas R (2017) Lipid mapping of the rat brain for models of disease. *Biochim Biophys Acta Biomembr* **1859**, 1548-1557.

[14] Wehrli PM, Ge J, Michno W, Koutarapu S, Dreos A, Jha D, Zetterberg H, Blennow K, Hanrieder J (2023) Correlative Chemical Imaging and Spatial Chemometrics Delineate Alzheimer Plaque Heterogeneity at High Spatial Resolution. *JACS Au* **3**, 762-774.

[15] Kaya I, Jennische E, Dunevall J, Lange S, Ewing AG, Malmberg P, Baykal AT, Fletcher JS (2020) Spatial Lipidomics Reveals Region and Long Chain Base Specific Accumulations of Monosialogangliosides in Amyloid Plaques in Familial Alzheimer's Disease Mice (5xFAD) Brain. *ACS Chem Neurosci* **11**, 14-24.

[16] Zhang Q, Li Y, Sui P, Sun XH, Gao Y, Wang CY (2023) MALDI mass spectrometry imaging discloses the decline of sulfoglycosphingolipid and glycerophosphoinositol species in the brain regions related to cognition in a mouse model of Alzheimer's disease. *Talanta* **266**, 125022.

[17] Gonzalez de San Roman E, Llorente-Ovejero A, Martinez-Gardeazabal J, Moreno-Rodriguez M, Gimenez-Llort L, Manuel I, Rodriguez-Puertas R (2021) Modulation of Neurolipid Signaling and Specific Lipid Species in the Triple Transgenic Mouse Model of Alzheimer's Disease. *Int J Mol Sci* **22**.

[18] Llorente-Ovejero A, Martinez-Gardeazabal J, Moreno-Rodriguez M, Lombardero L, Gonzalez de San Roman E, Manuel I, Giralt MT, Rodriguez-Puertas R (2021) Specific Phospholipid Modulation by Muscarinic Signaling in a Rat Lesion Model of Alzheimer's Disease. *ACS Chem Neurosci* **12**, 2167-2181.

[19] Gonzalez de San Roman E, Manuel I, Giralt MT, Ferrer I, Rodriguez-Puertas R (2017) Imaging mass spectrometry (IMS) of cortical lipids from preclinical to severe stages of Alzheimer's disease. *Biochim Biophys Acta Biomembr* **1859**, 1604-1614.

[20] Yuki D, Sugiura Y, Zaima N, Akatsu H, Takei S, Yao I, Maesako M, Kinoshita A, Yamamoto T, Kon R, Sugiyama K, Setou M (2014) DHA-PC and PSD-95 decrease after loss of synaptophysin and before neuronal loss in patients with Alzheimer's disease. *Sci Rep* **4**, 7130.

[21] Grimm MO, Grosgen S, Riemenschneider M, Tanila H, Grimm HS, Hartmann T (2011) From brain to food: analysis of phosphatidylcholins, lyso-phosphatidylcholins and phosphatidylcholin-plasmalogens derivates in Alzheimer's disease human post mortem brains and mice model via mass spectrometry. *J Chromatogr A* **1218**, 7713-7722.

[22] Buckner RL, Andrews-Hanna JR, Schacter DL (2008) The brain's default network: anatomy, function, and relevance to disease. *Ann N Y Acad Sci* **1124**, 1-38.

[23] Mesulam MM (2013) Cholinergic circuitry of the human nucleus basalis and its fate in Alzheimer's disease. *J Comp Neurol* **521**, 4124-4144.

[24] Kao YC, Ho PC, Tu YK, Jou IM, Tsai KJ (2020) Lipids and Alzheimer's Disease. *Int J Mol Sci* **21**.

[25] Vance JE, Campenot RB, Vance DE (2000) The synthesis and transport of lipids for axonal growth and nerve regeneration. *Biochim Biophys Acta* **1486**, 84-96.

[26] Wurtman RJ (1992) Choline metabolism as a basis for the selective vulnerability of cholinergic neurons. *Trends Neurosci* **15**, 117-122.

[27] Selley DE, Welch SP, Sim-Selley LJ (2013) Sphingosine lysolipids in the CNS: endogenous cannabinoid antagonists or a parallel pain modulatory system? *Life Sci* **93**, 187-193.

[28] Hla T (2004) Physiological and pathological actions of sphingosine 1-phosphate. *Semin Cell Dev Biol* **15**, 513-520.

[29] Di Marzo V, Bisogno T, De Petrocellis L, Melck D, Martin BR (1999) Cannabimimetic fatty acid derivatives: the anandamide family and other endocannabinoids. *Curr Med Chem* **6**, 721-744.

[30] Llorente-Ovejero A, Manuel I, Giralt MT, Rodriguez-Puertas R (2017) Increase in cortical endocannabinoid signaling in a rat model of basal forebrain cholinergic dysfunction. *Neuroscience* **362**, 206-218.
[31] Gessa GL, Casu MA, Carta G, Mascia MS (1998) Cannabinoids decrease acetylcholine release in the medial-prefrontal cortex and hippocampus, reversal by SR 141716A. *Eur J Pharmacol* **355**, 119-124.
[32] Garzon M, Chan J, Mackie K, Pickel VM (2022) Prefrontal cortical distribution of muscarinic M2 and cannabinoid-1 (CB1) receptors in adult male mice with or without chronic adolescent exposure to Delta9-tetrahydrocannabinol. *Cereb Cortex* **32**, 5420-5437.
[33] Garzon M, Wang G, Chan J, Bourie F, Mackie K, Pickel VM (2021) Adolescent administration of Delta(9)-THC decreases the expression and function of muscarinic-1 receptors in prelimbic prefrontal cortical neurons of adult male mice. *IBRO Neurosci Rep* **11**, 144-155.
[34] Fernandez-Moncada I, Eraso-Pichot A, Dalla Tor T, Fortunato-Marsol B, Marsicano G (2023) An enquiry to the role of CB1 receptors in neurodegeneration. *Neurobiol Dis* **184**, 106235.
[35] Estrada JA, Contreras I (2020) Endocannabinoid Receptors in the CNS: Potential Drug Targets for the Prevention and Treatment of Neurologic and Psychiatric Disorders. *Curr Neuropharmacol* **18**, 769-787.
[36] Manuel I, Gonzalez de San Roman E, Giralt MT, Ferrer I, Rodriguez-Puertas R (2014) Type-1 cannabinoid receptor activity during Alzheimer's disease progression. *J Alzheimers Dis* **42**, 761-766.
[37] Ramirez BG, Blazquez C, Gomez del Pulgar T, Guzman M, de Ceballos ML (2005) Prevention of Alzheimer's disease pathology by cannabinoids: neuroprotection mediated by blockade of microglial activation. *J Neurosci* **25**, 1904-1913.
[38] Ahmad R, Goffin K, Van den Stock J, De Winter FL, Cleeren E, Bormans G, Tournoy J, Persoons P, Van Laere K, Vandenbulcke M (2014) In vivo type 1 cannabinoid receptor availability in Alzheimer's disease. *Eur Neuropsychopharmacol* **24**, 242-250.
[39] Ceccom J, Loukh N, Lauwers-Cances V, Touriol C, Nicaise Y, Gentil C, Uro-Coste E, Pitson S, Maurage CA, Duyckaerts C, Cuvillier O, Delisle MB (2014) Reduced sphingosine kinase-1 and enhanced sphingosine 1-phosphate lyase expression demonstrate deregulated sphingosine 1-phosphate signaling in Alzheimer's disease. *Acta Neuropathol Commun* **2**, 12.
[40] Schmitt FA, Nelson PT, Abner E, Scheff S, Jicha GA, Smith C, Cooper G, Mendiondo M, Danner DD, Van Eldik LJ, Caban-Holt A, Lovell MA, Kryscio RJ (2012) University of Kentucky Sanders-Brown healthy brain aging volunteers: donor characteristics, procedures and neuropathology. *Curr Alzheimer Res* **9**, 724-733.
[41] Mufson EJ, Chen EY, Cochran EJ, Beckett LA, Bennett DA, Kordower JH (1999) Entorhinal cortex beta-amyloid load in individuals with mild cognitive impairment. *Exp Neurol* **158**, 469-490.
[42] Folstein MF, Folstein SE, McHugh PR (1975) "Mini-mental state". A practical method for grading the cognitive state of patients for the clinician. *J Psychiatr Res* **12**, 189-198.
[43] Morris JC, Heyman A, Mohs RC, Hughes JP, van Belle G, Fillenbaum G, Mellits ED, Clark C (1989) The Consortium to Establish a Registry for Alzheimer's Disease (CERAD). Part I. Clinical and neuropsychological assessment of Alzheimer's disease. *Neurology* **39**, 1159-1165.
[44] SMITH A (1984) Symbol Digit Modalities Test manual-R. *Western Psychological, Los Angeles.*
[45] WECHSLER D (1987) Wechsler Memory Scale-Revised Manual. *Psychological Corporation, New York.*
[46] GOODGLASS H (1972) Kaplan. Assessment of aphasia and related disorders. *Lea & Febiger, Philadelphia*.
[47] Benton AL, Varney NR, Hamsher KD (1978) Visuospatial judgment. A clinical test. *Arch Neurol* **35**, 364-367.
[48] RAVEN. J.C. JHC, AND J. RAVEN (1992) Standard progressive matrices-1992 edition; Raven manual: Section 3. *Oxford Psychologists Press, Oxford*.
[49] Pittman J, Andrews H, Tatemichi T, Link B, Struening E, Stern Y, Mayeux R (1992) Diagnosis of dementia in a heterogeneous population. A comparison of paradigm-based diagnosis and physician's diagnosis. *Arch Neurol* **49**, 461-467.
[50] Stern Y, Gurland B, Tatemichi TK, Tang MX, Wilder D, Mayeux R (1994) Influence of education and occupation on the incidence of Alzheimer's disease. *JAMA* **271**, 1004-1010.

[51] McKhann G, Drachman D, Folstein M, Katzman R, Price D, Stadlan EM (1984) Clinical diagnosis of Alzheimer's disease: report of the NINCDS-ADRDA Work Group under the auspices of Department of Health and Human Services Task Force on Alzheimer's Disease. *Neurology* **34**, 939-944.
[52] Devanand DP, Folz M, Gorlyn M, Moeller JR, Stern Y (1997) Questionable dementia: clinical course and predictors of outcome. *J Am Geriatr Soc* **45**, 321-328.
[53] Ebly EM, Hogan DB, Parhad IM (1995) Cognitive impairment in the nondemented elderly. Results from the Canadian Study of Health and Aging. *Arch Neurol* **52**, 612-619.
[54] Petersen RC, Smith GE, Ivnik RJ, Tangalos EG, Schaid DJ, Thibodeau SN, Kokmen E, Waring SC, Kurland LT (1995) Apolipoprotein E status as a predictor of the development of Alzheimer's disease in memory-impaired individuals. *JAMA* **273**, 1274-1278.
[55] Perez SE, Getova DP, He B, Counts SE, Geula C, Desire L, Coutadeur S, Peillon H, Ginsberg SD, Mufson EJ (2012) Rac1b increases with progressive tau pathology within cholinergic nucleus basalis neurons in Alzheimer's disease. *Am J Pathol* **180**, 526-540.
[56] Braak H, Braak E (1991) Neuropathological stageing of Alzheimer-related changes. *Acta Neuropathol* **82**, 239-259.
[57] Newell KL, Hyman BT, Growdon JH, Hedley-Whyte ET (1999) Application of the National Institute on Aging (NIA)-Reagan Institute criteria for the neuropathological diagnosis of Alzheimer disease. *J Neuropathol Exp Neurol* **58**, 1147-1155.
[58] Mirra SS (1997) The CERAD neuropathology protocol and consensus recommendations for the postmortem diagnosis of Alzheimer's disease: a commentary. *Neurobiol Aging* **18**, S91-94.
[59] Robichaud G, Garrard KP, Barry JA, Muddiman DC (2013) MSiReader: an open-source interface to view and analyze high resolving power MS imaging files on Matlab platform. *J Am Soc Mass Spectrom* **24**, 718-721.
[60] Martinez-Gardeazabal J, Moreno-Rodriguez M, de San Roman EG, Abad B, Manuel I, Rodriguez-Puertas R (2023) Mass Spectrometry for the Advancement of Lipid Analysis in Alzheimer's Research. *Methods Mol Biol* **2561**, 245-259.
[61] Wishart DS, Feunang YD, Marcu A, Guo AC, Liang K, Vazquez-Fresno R, Sajed T, Johnson D, Li C, Karu N, Sayeeda Z, Lo E, Assempour N, Berjanskii M, Singhal S, Arndt D, Liang Y, Badran H, Grant J, Serra-Cayuela A, Liu Y, Mandal R, Neveu V, Pon A, Knox C, Wilson M, Manach C, Scalbert A (2018) HMDB 4.0: the human metabolome database for 2018. *Nucleic Acids Res* **46**, D608-D617.
[62] Angerer TB, Bour J, Biagi JL, Moskovets E, Frache G (2022) Evaluation of 6 MALDI-Matrices for 10 mum Lipid Imaging and On-Tissue MSn with AP-MALDI-Orbitrap. *J Am Soc Mass Spectrom* **33**, 760-771.
[63] Cheng H, Sun G, Yang K, Gross RW, Han X (2010) Selective desorption/ionization of sulfatides by MALDI-MS facilitated using 9-aminoacridine as matrix. *J Lipid Res* **51**, 1599-1609.
[64] Seyer A, Cantiello M, Bertrand-Michel J, Roques V, Nauze M, Bezirard V, Collet X, Touboul D, Brunelle A, Comera C (2013) Lipidomic and spatio-temporal imaging of fat by mass spectrometry in mice duodenum during lipid digestion. *PLoS One* **8**, e58224.
[65] Liu Y, Chen L, Qin L, Han M, Li J, Luo F, Xue K, Feng J, Zhou Y, Wang X (2019) Enhanced in situ detection and imaging of lipids in biological tissues by using 2,3-dicyanohydroquinone as a novel matrix for positive-ion MALDI-MS imaging. *Chem Commun (Camb)* **55**, 12559-12562.
[66] Fort PE, Rajendiran TM, Soni T, Byun J, Shan Y, Looker HC, Nelson RG, Kretzler M, Michailidis G, Roger JE, Gardner TW, Abcouwer SF, Pennathur S, Afshinnia F (2021) Diminished retinal complex lipid synthesis and impaired fatty acid beta-oxidation associated with human diabetic retinopathy. *JCI Insight* **6**.
[67] Mufson EJ, Malek-Ahmadi M, Perez SE, Chen K (2016) Braak staging, plaque pathology, and APOE status in elderly persons without cognitive impairment. *Neurobiol Aging* **37**, 147-153.
[68] Di Paolo G, Kim TW (2011) Linking lipids to Alzheimer's disease: cholesterol and beyond. *Nat Rev Neurosci* **12**, 284-296.
[69] Qian Z, Drewes LR (1991) Cross-talk between receptor-regulated phospholipase D and phospholipase C in brain. *FASEB J* **5**, 315-319.

[70] De Craene JO, Bertazzi DL, Bar S, Friant S (2017) Phosphoinositides, Major Actors in Membrane Trafficking and Lipid Signaling Pathways. *Int J Mol Sci* **18**.
[71] Kim SH, Yang JS, Lee JC, Lee JY, Lee JY, Kim E, Moon MH (2018) Lipidomic alterations in lipoproteins of patients with mild cognitive impairment and Alzheimer's disease by asymmetrical flow field-flow fractionation and nanoflow ultrahigh performance liquid chromatography-tandem mass spectrometry. *J Chromatogr A* **1568**, 91-100.
[72] Wood PL, Barnette BL, Kaye JA, Quinn JF, Woltjer RL (2015) Non-targeted lipidomics of CSF and frontal cortex grey and white matter in control, mild cognitive impairment, and Alzheimer's disease subjects. *Acta Neuropsychiatr* **27**, 270-278.
[73] Rodriguez-Puertas R, Pascual J, Vilaro T, Pazos A (1997) Autoradiographic distribution of M1, M2, M3, and M4 muscarinic receptor subtypes in Alzheimer's disease. *Synapse* **26**, 341-350.
[74] Mash DC, Flynn DD, Potter LT (1985) Loss of M2 muscarine receptors in the cerebral cortex in Alzheimer's disease and experimental cholinergic denervation. *Science* **228**, 1115-1117.
[75] Flynn DD, Ferrari-DiLeo G, Levey AI, Mash DC (1995) Differential alterations in muscarinic receptor subtypes in Alzheimer's disease: implications for cholinergic-based therapies. *Life Sci* **56**, 869-876.
[76] Willars GB, Nahorski SR, Challiss RA (1998) Differential regulation of muscarinic acetylcholine receptor-sensitive polyphosphoinositide pools and consequences for signaling in human neuroblastoma cells. *J Biol Chem* **273**, 5037-5046.
[77] Lyeth BG, Gong QZ, Dhillon HS, Prasad MR (1996) Effects of muscarinic receptor antagonism on the phosphatidylinositol bisphosphate signal transduction pathway after experimental brain injury. *Brain Res* **742**, 63-70.
[78] Schmidt M, Nehls C, Rumenapp U, Jakobs KH (1996) m3 Muscarinic receptor-induced and Gi-mediated heterologous potentiation of phospholipase C stimulation: role of phosphoinositide synthesis. *Mol Pharmacol* **50**, 1038-1046.
[79] Kooijman EE, Burger KN (2009) Biophysics and function of phosphatidic acid: a molecular perspective. *Biochim Biophys Acta* **1791**, 881-888.
[80] Goni FM, Alonso A (1999) Structure and functional properties of diacylglycerols in membranes. *Prog Lipid Res* **38**, 1-48.
[81] Ganesan S, Shabits BN, Zaremberg V (2015) Tracking Diacylglycerol and Phosphatidic Acid Pools in Budding Yeast. *Lipid Insights* **8**, 75-85.
[82] Pathmasiri KC, Pergande MR, Tobias F, Rebiai R, Rosenhouse-Dantsker A, Bongarzone ER, Cologna SM (2020) Mass spectrometry imaging and LC/MS reveal decreased cerebellar phosphoinositides in Niemann-Pick type C1-null mice. *J Lipid Res* **61**, 1004-1013.
[83] Eichberg J, Dawson RM (1965) Polyphosphoinositides in myelin. *Biochem J* **96**, 644-650.
[84] Hiraide T, Ikegami K, Sakaguchi T, Morita Y, Hayasaka T, Masaki N, Waki M, Sugiyama E, Shinriki S, Takeda M, Shibasaki Y, Miyazaki S, Kikuchi H, Okuyama H, Inoue M, Setou M, Konno H (2016) Accumulation of arachidonic acid-containing phosphatidylinositol at the outer edge of colorectal cancer. *Sci Rep* **6**, 29935.
[85] Lee HC, Inoue T, Imae R, Kono N, Shirae S, Matsuda S, Gengyo-Ando K, Mitani S, Arai H (2008) Caenorhabditis elegans mboa-7, a member of the MBOAT family, is required for selective incorporation of polyunsaturated fatty acids into phosphatidylinositol. *Mol Biol Cell* **19**, 1174-1184.
[86] Salem N, Jr., Wegher B, Mena P, Uauy R (1996) Arachidonic and docosahexaenoic acids are biosynthesized from their 18-carbon precursors in human infants. *Proc Natl Acad Sci U S A* **93**, 49-54.
[87] Zhang HQ, Chau ACM, Shea YF, Chiu PK, Bao YW, Cao P, Mak HK (2023) Disrupted Structural White Matter Network in Alzheimer's Disease Continuum, Vascular Dementia, and Mixed Dementia: A Diffusion Tensor Imaging Study. *J Alzheimers Dis* **94**, 1487-1502.
[88] Zhou Y, Wei L, Gao S, Wang J, Hu Z (2023) Characterization of diffusion magnetic resonance imaging revealing relationships between white matter disconnection and behavioral disturbances in mild cognitive impairment: a systematic review. *Front Neurosci* **17**, 1209378.

[89] Chang S, Varadarajan D, Yang J, Chen IA, Kura S, Magnain C, Augustinack JC, Fischl B, Greve DN, Boas DA, Wang H (2022) Scalable mapping of myelin and neuron density in the human brain with micrometer resolution. *Sci Rep* **12**, 363.

[90] Tan SS, Kalloniatis M, Truong HT, Binder MD, Cate HS, Kilpatrick TJ, Hammond VE (2009) Oligodendrocyte positioning in cerebral cortex is independent of projection neuron layering. *Glia* **57**, 1024-1030.

[91] Song H, McEwen HP, Duncan T, Lee JY, Teo JD, Don AS (2021) Sphingosine kinase 2 is essential for remyelination following cuprizone intoxication. *Glia* **69**, 2863-2881.

[92] Tomas-Roig J, Agbemenyah HY, Celarain N, Quintana E, Ramio-Torrenta L, Havemann-Reinecke U (2020) Dose-dependent effect of cannabinoid WIN-55,212-2 on myelin repair following a demyelinating insult. *Sci Rep* **10**, 590.

[93] He X, Huang Y, Li B, Gong CX, Schuchman EH (2010) Deregulation of sphingolipid metabolism in Alzheimer's disease. *Neurobiol Aging* **31**, 398-408.

[94] Couttas TA, Kain N, Daniels B, Lim XY, Shepherd C, Kril J, Pickford R, Li H, Garner B, Don AS (2014) Loss of the neuroprotective factor Sphingosine 1-phosphate early in Alzheimer's disease pathogenesis. *Acta Neuropathol Commun* **2**, 9.

[95] Chen C (2023) Inhibiting degradation of 2-arachidonoylglycerol as a therapeutic strategy for neurodegenerative diseases. *Pharmacol Ther* **244**, 108394.

[96] Hurst DP, Schmeisser M, Reggio PH (2013) Endogenous lipid activated G protein-coupled receptors: emerging structural features from crystallography and molecular dynamics simulations. *Chem Phys Lipids* **169**, 46-56.

[97] Hait NC, Maiti A (2017) The Role of Sphingosine-1-Phosphate and Ceramide-1-Phosphate in Inflammation and Cancer. *Mediators Inflamm* **2017**, 4806541.

[98] Sanchez C, Rueda D, Segui B, Galve-Roperh I, Levade T, Guzman M (2001) The CB(1) cannabinoid receptor of astrocytes is coupled to sphingomyelin hydrolysis through the adaptor protein fan. *Mol Pharmacol* **59**, 955-959.

[99] Rahman SA, Gathungu RM, Marur VR, St Hilaire MA, Scheuermaier K, Belenky M, Struble JS, Czeisler CA, Lockley SW, Klerman EB, Duffy JF, Kristal BS (2023) Age-related changes in circadian regulation of the human plasma lipidome. *Commun Biol* **6**, 756.

[100] Yang S, Park JH, Lu HC (2023) Axonal energy metabolism, and the effects in aging and neurodegenerative diseases. *Mol Neurodegener* **18**, 49.

[101] Stahon KE, Bastian C, Griffith S, Kidd GJ, Brunet S, Baltan S (2016) Age-Related Changes in Axonal and Mitochondrial Ultrastructure and Function in White Matter. *J Neurosci* **36**, 9990-10001.

[102] Lee JY, Harney DJ, Teo JD, Kwok JB, Sutherland GT, Larance M, Don AS (2023) The major TMEM106B dementia risk allele affects TMEM106B protein levels, fibril formation, and myelin lipid homeostasis in the ageing human hippocampus. *Mol Neurodegener* **18**, 63.

[103] Shokhirev MN, Johnson AA (2022) An integrative machine-learning meta-analysis of high-throughput omics data identifies age-specific hallmarks of Alzheimer's disease. *Ageing Res Rev* **81**, 101721.

[104] Chew H, Solomon VA, Fonteh AN (2020) Involvement of Lipids in Alzheimer's Disease Pathology and Potential Therapies. *Front Physiol* **11**, 598.

[105] Blank M, Enzlein T, Hopf C (2022) LPS-induced lipid alterations in microglia revealed by MALDI mass spectrometry-based cell fingerprinting in neuroinflammation studies. *Sci Rep* **12**, 2908.

[106] Jarmusch AK, Alfaro CM, Pirro V, Hattab EM, Cohen-Gadol AA, Cooks RG (2016) Differential Lipid Profiles of Normal Human Brain Matter and Gliomas by Positive and Negative Mode Desorption Electrospray Ionization - Mass Spectrometry Imaging. *PLoS One* **11**, e0163180.

[107] Rothman SM, Tanis KQ, Gandhi P, Malkov V, Marcus J, Pearson M, Stevens R, Gilliland J, Ware C, Mahadomrongkul V, O'Loughlin E, Zeballos G, Smith R, Howell BJ, Klappenbach J, Kennedy M, Mirescu C (2018) Human Alzheimer's disease gene expression signatures and immune profile in APP mouse models: a discrete transcriptomic view of Abeta plaque pathology. *J Neuroinflammation* **15**, 256.

[108] Blank M, Hopf C (2021) Spatially resolved mass spectrometry analysis of amyloid plaque-associated lipids. *J Neurochem* **159**, 330-342.

[109] Ge J, Koutarapu S, Jha D, Dulewicz M, Zetterberg H, Blennow K, Hanrieder J (2023) Tetramodal Chemical Imaging Delineates the Lipid-Amyloid Peptide Interplay at Single Plaques in Transgenic Alzheimer's Disease Models. *Anal Chem* **95**, 4692-4702.

[110] Michno W, Wehrli PM, Koutarapu S, Marsching C, Minta K, Ge J, Meyer SW, Zetterberg H, Blennow K, Henkel C, Oetjen J, Hopf C, Hanrieder J (2022) Structural amyloid plaque polymorphism is associated with distinct lipid accumulations revealed by trapped ion mobility mass spectrometry imaging. *J Neurochem* **160**, 482-498.

[111] Mufson EJ, Binder L, Counts SE, DeKosky ST, de Toledo-Morrell L, Ginsberg SD, Ikonomovic MD, Perez SE, Scheff SW (2012) Mild cognitive impairment: pathology and mechanisms. *Acta Neuropathol* **123**, 13-30.

[112] Bennett DA, Wilson RS, Boyle PA, Buchman AS, Schneider JA (2012) Relation of neuropathology to cognition in persons without cognitive impairment. *Ann Neurol* **72**, 599-609.

[113] DeKosky ST, Ikonomovic MD, Styren SD, Beckett L, Wisniewski S, Bennett DA, Cochran EJ, Kordower JH, Mufson EJ (2002) Upregulation of choline acetyltransferase activity in hippocampus and frontal cortex of elderly subjects with mild cognitive impairment. *Ann Neurol* **51**, 145-155.

[114] Davis KL, Mohs RC, Marin D, Purohit DP, Perl DP, Lantz M, Austin G, Haroutunian V (1999) Cholinergic markers in elderly patients with early signs of Alzheimer disease. *JAMA* **281**, 1401-1406.

[115] Bennett DA, Schneider JA, Wilson RS, Bienias JL, Arnold SE (2004) Neurofibrillary tangles mediate the association of amyloid load with clinical Alzheimer disease and level of cognitive function. *Arch Neurol* **61**, 378-384.

Table 1. Demographic, Cognitive, and Neuropathological Variables Stratified by Clinical Group.

	YAC (n=6)	NCI (n = 5)	MCI (n = 5)	AD (n = 5)	P-value	Groupwise Comparisons
Age at Death (years) (range)	68.83±7.94 (58-79)	86.27±4.85 (79-90)	83.32±7.44 (72-92)	92.04±8.54 (80-101)	0.004	YAC<NCI
Education (years) (range)	n/a	18.60±2.97 (15, 22)	19.60±1.82 (18, 22)	17.80±3.11 (14, 21)	0.69	ns
Sex (M/F)	4/2	1/4	2/3	2/3	0.74	ns
APOE ε4 (Carrier/Non-Carrier)	n/a	1/4	0/5	2/3	0.29	ns
MMSE (range)	n/a	27.80±0.84 (27, 29)	28.2±2.17 (25, 30)	17.80±4.15 (15, 24)	0.008	NCI, MCI>AD
Global Cognitive Score (z-score) (range)	n/a	0.04±0.27 (-0.24, 0.43)	-0.29±0.43 (-0.95, 0.15)	-1.36±1.01 (-2.45, 0.08)	0.05	NCI>AD
Episodic Memory (z-score) (range)	n/a	0.39±0.39 (-0.17, 0.85)	-0.24±0.86 (-1.46, 0.93)	-1.67±1.35 (-3.0, 0.07)	0.04	NCI>AD
Semantic Memory (z-score) (range)	n/a	-0.39±0.87 (-1.30, 0.59)	-0.30±0.48 (-0.84, 0.20)	-1.14±0.82 (-2.21, 0.06)	0.22	ns
Working Memory (z-score) (range)	n/a	0.16±0.27 (-0.19, 0.47)	-0.74±0.39 (-1.17, -0.17)	-1.00±1.14 (-2.14, 0.56)	0.07	ns
Perceptual Speed (z-score) (range)	n/a	-0.09±0.61 (-0.85, 0.42)	-0.39±0.35 (-0.99, -0.13)	-2.33±0.79 (-3.38, -1.43)	0.008	NCI>AD
Visuospatial (z-score) (range)	n/a	-0.19±0.78 (-0.61, 1.02)	-0.32±0.27 (-0.61, -0.02)	-0.82±1.31 (-2.12, 0.75)	0.75	ns
Post-Mortem Interval (hours) (range)	10.29±5.52 (4.8, 21)	4.67±1.86 (3, 9.9)	5.73±2.99 (2.4, 6.9)	5.53±3.79 (2.6, 12)	0.19	ns
Brain Weight (grams) (range)	1,235±122* (1100, 1375)	1,186±93.05 (1040, 1380)	1,192±133.68 (1095, 1310)	1,158±126.57 (1020, 1340)	0.75	ns
Braak Stage						
I-II	0	1	3	0	0.15	ns
III-IV	0	4	1	3		
V-VI	0	0	1	2		
CERAD						
No AD	n/a	2	3	0	0.09	ns
Possible AD		0	0	0		
Probable AD		3	0	3		
Definite AD		0	2	2		
NIA Reagan						
Not AD	n/a	0	0	0	0.20	ns
Low Likelihood		2	3	0		
Intermediate Likelihood		3	1	3		
High Likelihood		0	1	2		

*n=5, n/a: not applicable, ns: non-significant

Table 2. [^{35}S]GTPγS binding induced by WIN55,212-2 (10 µM), CYM-5442 (10 µM) and Carbachol (100 µM) in frontal cortex lamina and white matter of NCI, MCI and AD expressed in nCi/g t.e.

Brain region	NCI	MCI	AD
	CB1 receptor activity (nCi/g t.e.)		
Grey matter	260 ± 135	399.7 ± 176	402.1 ± 199
Layer I-II	179 ± 95	279 ± 114	512 ± 317
Layer III-IV	493 ± 228	383.7 ± 196	373.1 ± 208
Layer V-VI	420 ± 84	539.1 ± 130	700.2 ± 117*****
White matter	44.73 ± 33.54	77.2 ± 113	50.9 ± 29
	S1P1 receptor activity (nCi/g t.e.)		
Grey matter	1267 ± 309	1384 ± 309	1069 ± 379
Layer I-II	908 ± 446	921.9 ± 208	983.9 ± 315
Layer III-IV	1097 ± 358	1369 ± 535	1156 ± 426
Layer V-VI	1509 ± 288	1560 ± 405	1330 ± 404
White matter	662.9 ± 271	365.6 ± 148	224.3 ± 92*****
	M2/M4 receptor activity (nCi/g t.e.)		
Grey matter	146 ± 51	356 ± 91	70 ± 49##
Layer I-II	158 ± 113	144 ± 190	36 ± 62
Layer III-IV	142 ± 77	348 ± 189	180 ± 100
Layer V-VI	149 ± 83	335 ± 210	57 ± 25#
White matter	85 ± 82	77 ± 113	51 ± 29

Data is presented as the mean ± SEM, *****p<0.05 AD *vs* NCI, ##p<0.01 AD *vs* MCI.

724 **Figure 1.**

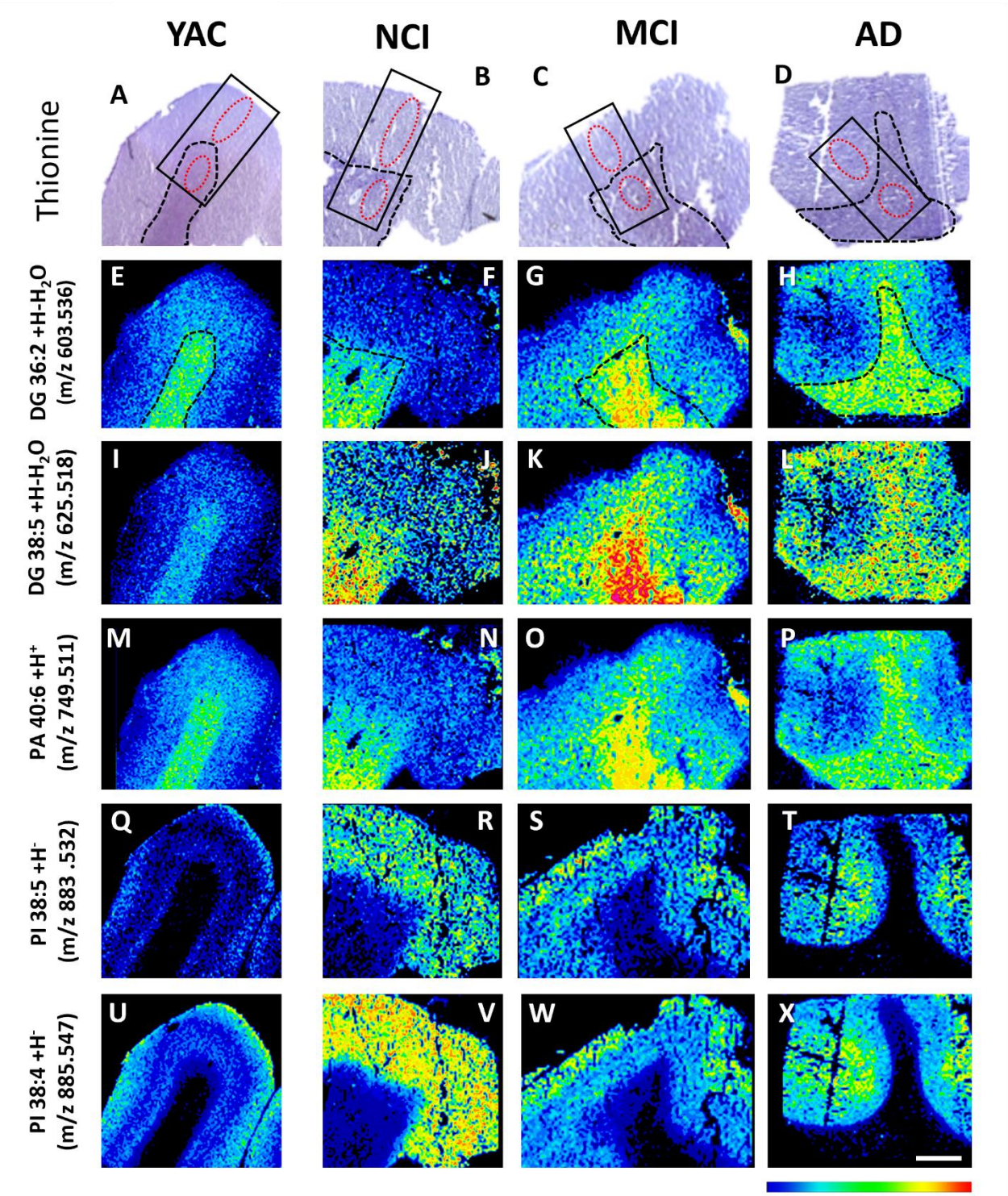

725

726

Figure 2.

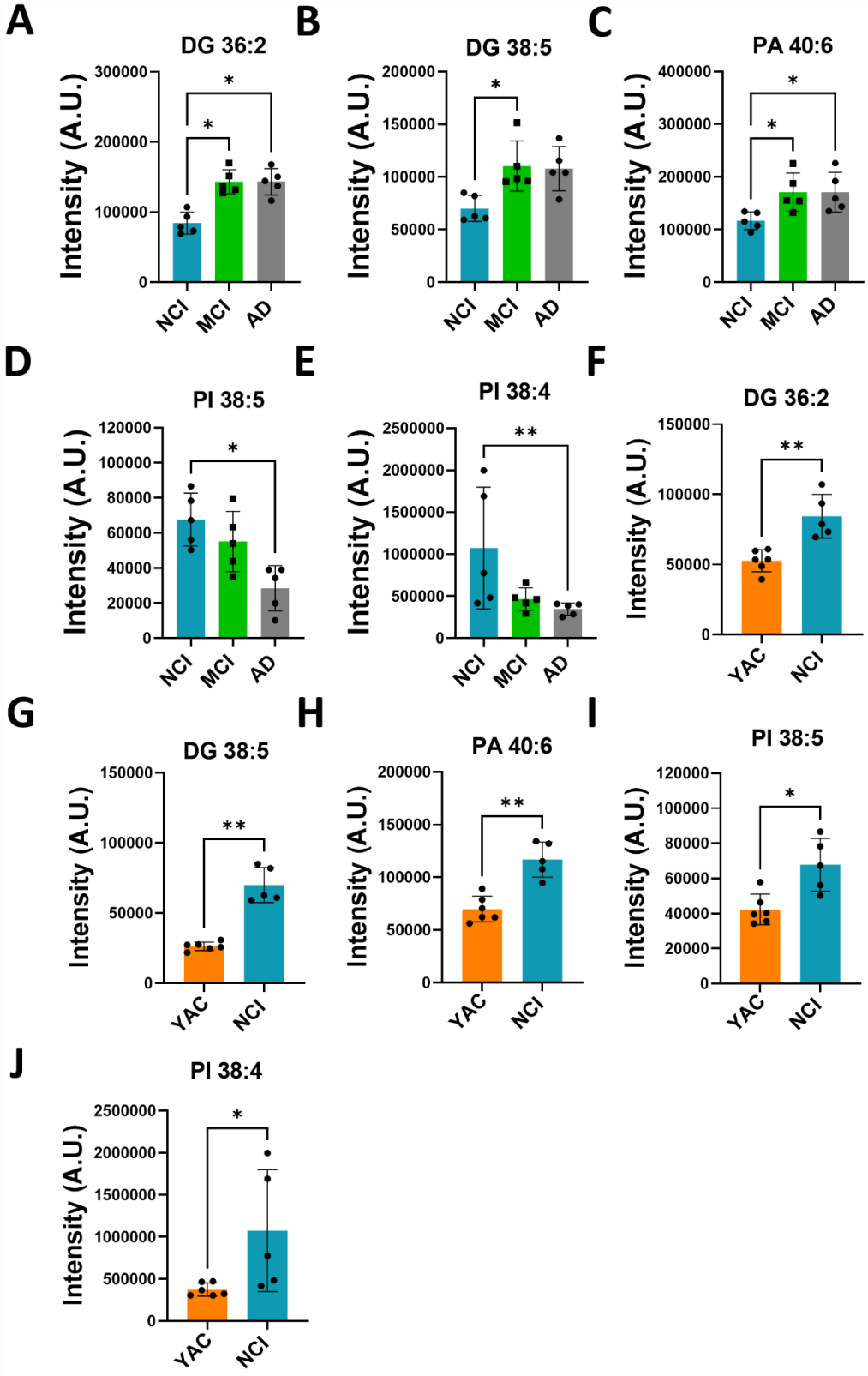
A
DG 36:2
Intensity (A.U.)
300000
200000
100000
0
NCI
MCI
AD
B
DG 38:5
200000
150000
100000
50000
C
PA 40:6
400000
300000
D
PI 38:5
120000
100000
80000
60000
40000
20000
E
PI 38:4
2500000
2000000
1500000
1000000
500000
F
DG 36:2
150000
50000
YAC
G
DG 38:5
H
PA 40:6
I
PI 38:5
J
PI 38:4

729 **Figure 3.**

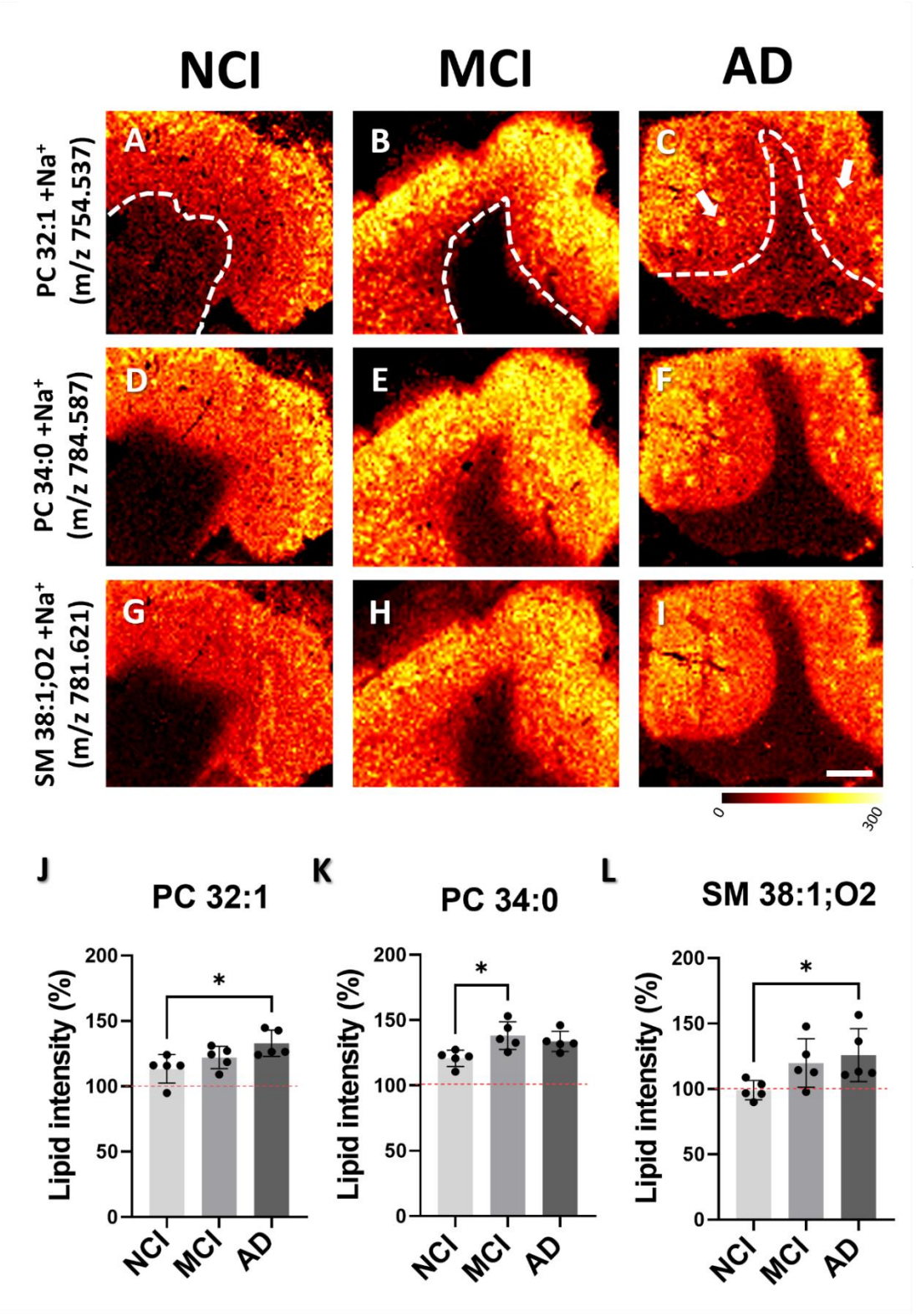

730

731

Figure 4.

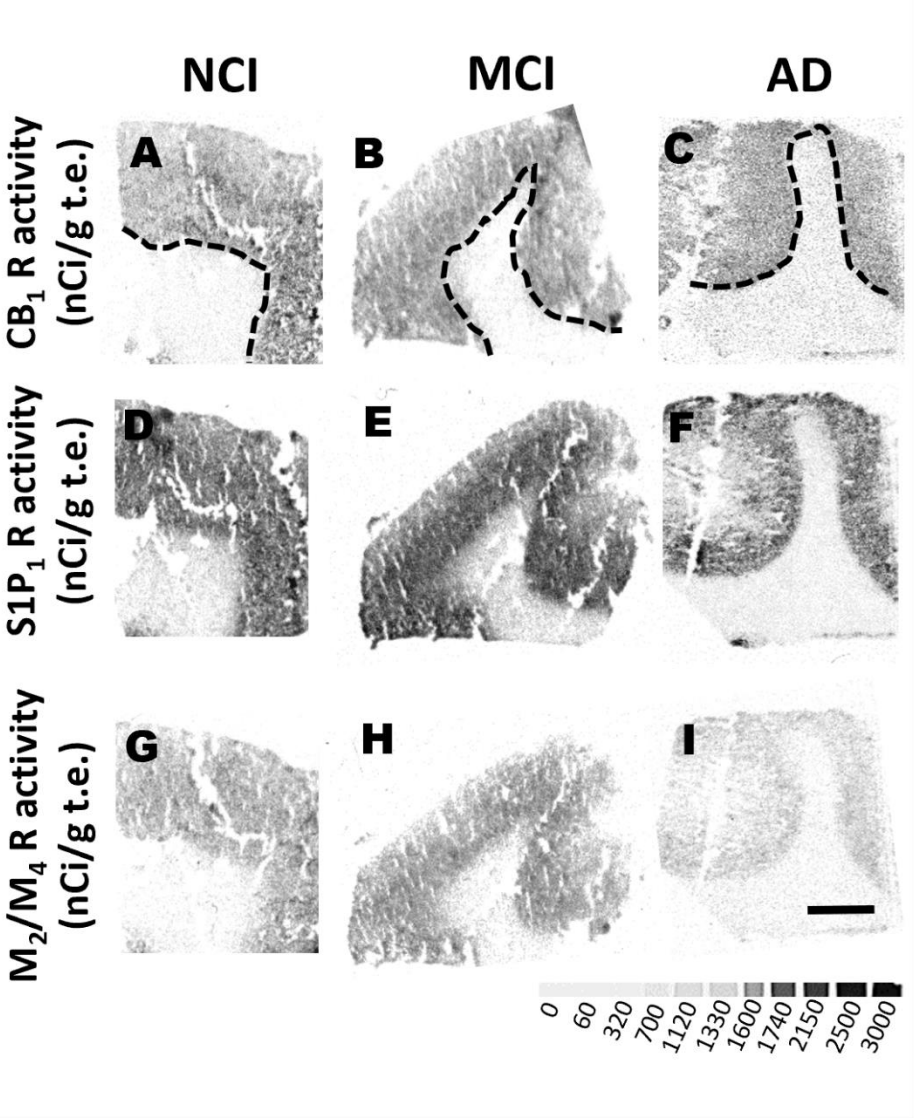
NCI
MCI
AD
CB1 R activity (nCi/g t.e.)
S1P1 R activity (nCi/g t.e.)
M2/M4 R activity (nCi/g t.e.)
A
B
C
D
E
F
G
H
I
0
60
320
700
1120
1330
1600
1740
2150
2500
3000

740 **Figure 5.**

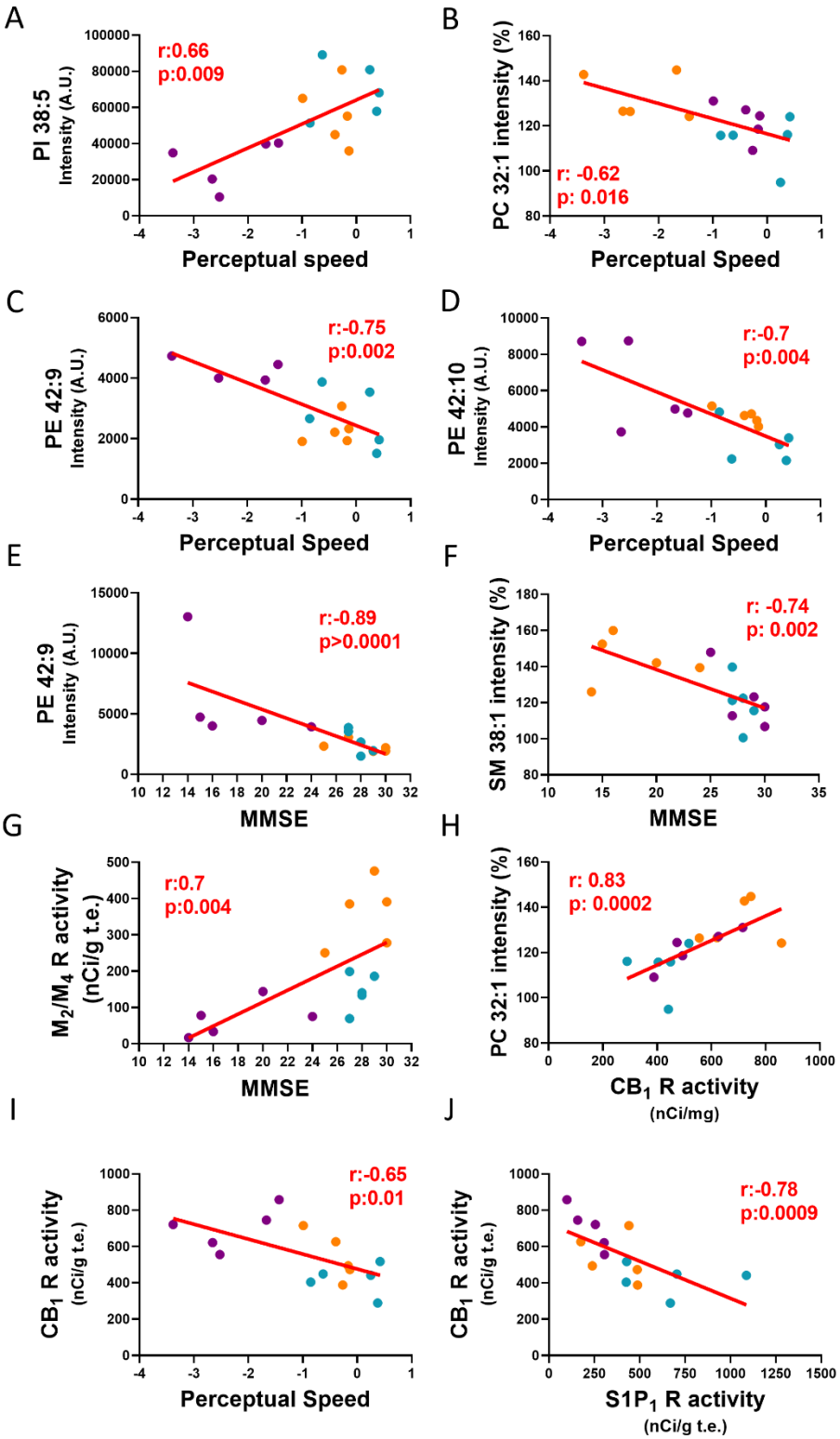

741

Figure legends

Fig. 1. Sections showing MALDI-MSI ion lipid species distribution counterstained with Thionine-showing significant differences in frontal cortex WM intensities between YAC, NCI, MCI and AD cases. In the thionine-stained sections the rectangle (black box) indicates the area scanned by MALDI-MSI and the red oval denotes the area exported for analysis from a YAC (A), NCI (B), MCI (C) and an AD (D) case. MALDI-MSI color images of the distribution of diacylglycerol (DG) 36:2 (E-H), 38:5 (I-L), phosphatidic acid (PA) 40:6 (M-P), phosphatidylinositol (PI) 38:5 (Q-T), 38:4 (U-X) in the FC. Note that all lipids displayed an increase in intensity in the older NCI (F, J, N, R and V) compared to YAC (E, I, M, Q and U) cases. WM intensity of DG 36:2, 38:5 and PA 40:6 was significantly higher in MCI (G, K and O) compared to NCI (F, J and N) cases while WM intensity of PI 38:5 and 38:4 was significantly lower in AD (T and X) compared to NCI (R and V). Scale bar = 4 mm. Multi-colored ion intensity scale values: DG 36:2 = 0 – 4 x 10^5 A.U, DG 38:5 = 0 – 2 x 10^5 A.U, PA 40:6 = 0 – 3 x 10^5 A.U, PI 38:5 = 0 – 2 x 10^5 A.U and PI 38:4 = 0 – 3 x 10^7 A.U.

Fig. 2. Histograms showing MALDI-MSI lipid intensity in frontal cortex WM for YAC, NCI, MCI and AD cases. (A-E) Significant differences of lipids, obtained by the average of absolute intensities in arbitrary units (A.U.) of WM between NCI, MCI and AD were shown in panels, while (F-J) significant differences between YAC and NCI were shown in panels. **$p<0.01$, *$p<0.05$. Abbreviations: DG = Diacylglycerol, PA = phosphatidic acid, PI = phosphatidylinositol.

Fig. 3. MALDI-MSI ion distribution images and histograms showing differences in the intensities of lipid patches in GM between NCI, MCI and AD cases. (A-C) GM images, above dashed line, show the distribution of PC 32:1, (D-F) SM 38:1 and (G-I) PC 34:0. (J-L) Histograms display percentage of changes in lipid intensity across NCI, MCI and AD cases. Percent change in lipid intensity was determined

764 by comparing areas within the GM with no accumulation (100 %) to those with lipid accumulations. Red
765 dashed line indicates background level. Scale bar in panel I = 4 mm. Multicolored scale bar below panel
766 I indicates changes in intensity level. Abbreviations: PC = phosphatidylcholine and SM = sphingomyelin.

767 **Fig. 4. Functional autoradiographic images of lipid related receptors.** Representative
768 autoradiographic images of frontal cortex activity for CB_1R (A-D), $S1P_1R$ (E-J) and M_2/M_4 activity
769 stimulated by WIN55,212-2, CYM-5442 and carbachol (K-L) showing differences in GTPγS binding in
770 GM and WM in NCI, MCI and AD cases. Dashed line differentiates GM from WM. Scale bar in I = 4
771 mm. Grayscale bar below panel I indicates levels of GTPγS binding (nCi/g t.e.).

772 **Fig. 5. Linear regression graphs show associations between lipids intensities, receptor activity and**
773 **cognitive performance tests.** (A) Associations between perceptual speed and PI 38:5 intensity A.U., (B)
774 PC 32:1 intensity (%), (C) PE 42:9 intensity A.U. (D) PE 42:10 intensity A.U. (E) MMSE and PE 42:9
775 intensity A.U., (F) SM 38:1 intensity (%), (G) M_2/M_4 receptor activity. (H) CB_1 receptor activity in GM
776 layers V-VI and PC 32:1 intensity (%), (I) perceptual speed and (J) $S1P_1$ receptor activity in WM. Blue
777 dots correspond to NCI, orange dots to MCI and purple dots to AD. Abbreviations: PI =
778 Phosphatidylinositol, PE = Phosphatidylethanolamine, PC = phosphatidylcholine and SM =
779 sphingomyelin.

780

781

782